Medizinische Fakultät
der
Universität Duisburg-Essen

aus der Klinik für Kinderheilkunde III

Die klinische Verwendung und der Nutzen von extrazellulären Vesikeln in der pädiatrischen akuten myeloischen Leukämie

I n a u g u r a l - D i s s e r t a t i o n
zur
Erlangung des Doktorgrades der Medizin
durch die Medizinische Fakultät
der Universität Duisburg-Essen

vorgelegt von

Fabienne Kunz
aus Essen

2021

DOI: 10.17185/duepublico/75389
URN: urn:nbn:de:hbz:465-20220330-090435-8

Dekan: Herr Univ.-Prof. Dr. med. J. Buer

1. Gutachter: Herr Prof. Dr. med. D. Reinhardt

2. Gutachter: Herr Priv.-Doz. Dr. med. M. Hanoun

Tag der mündlichen Prüfung: 29. November 2021

Überblick der Publikationen

Die Ergebnisse der vorliegenden Arbeit wurden veröffentlicht.

1. **Detection of AML-specific mutations in pediatric patient plasma using extracellular vesicle–derived RNA.**
   Kunz, F., Kontopoulou, E., Reinhardt, K., Soldierer, M., Strachan, S., Reinhardt, D., Thakur, B. K.
   Annals of Hematoly. Januar 2019; 98(3), 595-603.

2. **Evaluation of dsDNA from extracellular vesicles in pediatric AML diagnostics.**
   Kontopoulou, E., Strachan, S., Reinhardt, K., Kunz, F., Walter, C., Walkenfort, B., Jastrow, H., Hasenberg, M., Giebel, B., von Neuhoff, N., Reinhardt, D., Thakur, B.K.
   Annals of Hematology. Januar 2020; 99(3), 459-475.

Inhaltsverzeichnis

1 Einleitung 5
1.1 Akute myeloische Leukämie im Kindesalter 5
1.2 Diagnostik und Therapie der akuten myeloischen Leukämie 6
1.3 Mutationen 8
1.4 Extrazelluläre Vesikel 10
2. Ziel der Arbeit 13
3. Ergebnisse 14
3.1 Detection of AML-specific mutations in pediatric patient plasma using extracellular vesicle–derived RNA. 14
3.2 Evaluation of dsDNA from extracellular vesicles in pediatric AML diagnostics 24
4. Diskussion 42
4.1 Erfolgreiche Mutationsdetektion in EV-RNA der Zelllinien 42
4.2 RNA-Isolierung aus den EVs der pädiatrischen Plasmaproben 43
4.3 Analyse der EV-RNA der Patientenproben 44
4.4 Quantifizierung der EVs aus weiteren Patientenproben 45
4.5 Analyse der EV-DNA auf Mutationsstatus 45
4.6 Fazit 47
5. Zusammenfassung 49
6. Literaturverzeichnis 51
7. Abkürzungen 57
8. Liste der Abbildungen 59
9. Danksagung 60
10. Lebenslauf 61

1 Einleitung

1.1 Akute myeloische Leukämie im Kindesalter

Die akute myeloische Leukämie (AML) ist eine maligne Erkrankung des blutbildenden Systems, die durch die klonale Ausdehnung von unreifen, abnormalen, myeloischen Vorläuferzellen gekennzeichnet ist. Diese erwerben genetische Anomalien in zellulären Komponenten, welche an der Selbsterneuerung, Proliferation und Differenzierung beteiligt sind (Lonetti, Pession, & Masetti, 2019). Dass es sich bei der AML um eine heterogene Erkrankung handelt, zeigt sich in den Unterschieden der Morphologie, dem Immunphänotyp sowie in zytogenetischen und molekularen Aberrationen (Balgobind et al., 2011).

Pro Jahr erkranken in Deutschland etwa 100 Kinder unter 15 Jahren an der AML. Der Median des Erkrankungsalters bei unter 15-Jährigen liegt bei 6,3 Jahren. Die Inzidenz liegt bei 0,7 pro 100.000 Kindern mit einem Verhältnis von Mädchen zu Jungen von 1:1,1 (Kaatsch, 2016). Nach einer anfänglich hohen Inzidenz in den ersten beiden Lebensjahren, zeigt diese vorerst einen deutlichen Abfall, wohingegen sie ab dem 9. Lebensjahr erneut ansteigt (Creutzig et al., 2016).
Ursächlich für die Entstehung der AML sind in den meisten Fällen die zugrunde liegenden genetischen Veränderungen. Lediglich in 5 % der Fälle kann das Auftreten einer AML mit einer genetischen Prädisposition, einer intrauterinen Exposition mit Strahlung oder Substanzen, wie zum Beispiel Benzol oder unterschiedlichen Medikamenten assoziiert werden (Creutzig & Reinhardt, 2018).
Bei den genetischen Faktoren spielen vor allem Keimbahnveränderungen eine wesentliche Rolle, da Patienten mit kongenitalen Syndromen, wie zum Beispiel der Trisomie 21 ein bis zu 150-fach erhöhtes Risiko für das Auftreten einer AML aufweisen (Bhatnagar, Nizery, Tunstall, Vyas, & Roberts, 2016).

Zu den typischen Symptomen der AML gehören Blässe, Müdigkeit und Leistungsminderung, eine vermehrte Blutungsneigung zum Beispiel in Form von punktförmigen Einblutungen, sogenannten Petechien, sowie eine gesteigerte Infektanfälligkeit mit Fieber. Die beschriebenen Symptome lassen sich im Rahmen der

Knochenmarkinsuffizienz erklären, welche eine Panzytopenie, das heißt eine Zellarmut aller drei Zellreihen (Erythrozyten, Thrombozyten und Granulozyten), verursacht. Hinzu können neben vergrößerten Lymphknoten eine Hepato- und/ oder Splenomegalie als Bauchtumoren imponieren. 20 % der Patienten klagen darüber hinaus über Gelenk- und Knochenschmerzen (Creutzig, Dworzak & Reinhardt, 2019).

1.2 Diagnostik und Therapie der akuten myeloischen Leukämie

Die bei Verdacht durchzuführende Initialdiagnostik, dient neben der Diagnosesicherung auch der Risikostratifizierung der Patienten, welche für die Therapieentscheidung nötig ist. Für diese Initialdiagnostik sind neben einer detaillierten Anamnese, einer körperlichen Untersuchung und einer Blutbild- sowie Differenzialblutbildbestimmung, Nativ-Ausstriche des Blutes und des Knochenmarks (KM) zur Beurteilung der Zellmorphologie notwendig. Hierbei ist eine Knochenmarkpunktion für die Gewinnung des Materials essenziell. Um einen Befall des zentralen Nervensystems (ZNS) ausschließen zu können, muss bei gegebenen Hinweisen zudem eine initiale Liquorpunktion erfolgen. Im Anschluss können noch ergänzende Untersuchungen, wie beispielsweise bildgebende Verfahren oder Ultraschalluntersuchungen durchgeführt werden (Creutzig, Dworzak & Reinhardt, 2019).

Die Einteilung der AML erfolgt durch die WHO-Klassifikation 2016. Anhand zytogenetischer, molekulargenetischer und morphologischer Merkmale kann die Unterteilung in die Subtypen erfolgen (Arber et al., 2016). Die Morphologie lässt sich weitestgehend nach der früheren FAB (French-American-British)-Klassifikation beschreiben, die von einer Französisch-Britisch-Amerikanischen Arbeitsgruppe im Jahre 1976 publiziert wurde (Bennett et al., 1976). Die FAB-Subtypen stellen im klinischen Alltag eine große Relevanz dar, da sie zur Erkennung der akuten Promyelozytenleukämie (PML) obligat sind und sich die Behandlung der PML deutlich von den anderen Leukämieformen unterscheidet (Creutzig & Reinhardt, 2018).

Die Beurteilung der Zytologie erfolgt durch den KM-Ausstrich in Verbindung mit dem Blutbild. Hierbei muss der Anteil an Blasten im KM an den kernhaltigen Zellen zur Diagnosesicherung der AML ≥30% betragen. Im Anschluss daran wird die Methode der Zytochemie angewandt.

Hierbei werden die Zellen mit verschiedenen Färbemethoden eingefärbt und mikroskopisch beurteilt (Creutzig, Dworzak & Reinhardt, 2019).

Zur Abgrenzung verschiedener AML-Subtypen erfolgt die Immunphänotypisierung. Hierfür werden verschiedene Antigene verwendet, die sich auf der Oberfläche der Blasten oder im Zytoplasma finden lassen (Creutzig & Reinhardt, 2018).

Prognostic Group by Genetics	Definition
Favorable[a]	t(8;21)(q22;q22)/*RUNX1-RUNX1T1* inv(16)(p13.1q22) or t(16;16)(p13.1;q22)/*CBFB-MYH11* t(15;17)(q22;q12)/*PML-RARA*
Intermediate (other)	Cytogenetic abnormalities not classified as favorable or unfavorable, including *MLL* aberration t(9;11)(p22;q23)/*MLL-MLLT3*
Unfavorable[b]	−7, −5, or structural aberrations of 5p or 5q inv(3)(q21q26.2) or t(3;3)(q21;q26.2)/ *GATA2-MECOM* or other *3q26/MECOM* rearrangements t(6;9)(p23;q34)/*DEK-NUP214* Complex karyotype (≥3 abnormalities) 12p abnormalities 17p abnormalities Other 11q23/*MLL* aberrrations[c]

Abbreviations: AML, acute myeloid leukemia; CBFB, core-binding factor β; ELL, RNA polymerase II elongation factor; GATA2, GATA binding protein 2; MECOM, MDS1 and EVI1 complex locus; MLL, mixed-lineage leukemia; MYH11, myosin heavy chain 11; NPM1, nucleophosmin; NUP214, nucleoporin 214; PML, promyelocytic leukemia; RARA, retinoic acid receptor α; RUNX, runt-related transcription factor 1.

[a]Not considered: molecular in normal-karyotype AML, *NPM1*-mutated AML, *FLT3*-negative, *CEBPA* double mutation, and t(1;11)(q21;q23)/*MLL-MLLT11*(AF1Q).

[b]Excluding cases with a favorable karyotype.

[c]Other 11q23 aberrations include t(11;19)(q23;p13.1)/*MLL-ELL* and t(11;19)(q23;p13.3)/*MLL-MLLT1*, which are classified as unfavorable in adults by the European LeukemiaNet but as intermediate by others.[7,13]

Abbildung 1 **Definitionen von prognostischen Gruppen aufgrund ihrer Genetik** (Creutzig et al., 2016).

Creutzig et al. veröffentliche bereits 2016 eine Tabelle, welche drei prognostische AML-Subgruppen definiert (siehe Abbildung 1). Sie enthalten die derzeit bereits mit AML-assoziierten Mutationen, und werden in Standardrisiko, intermediäres Risiko und

Hochrisiko für die Einschätzung des Therapieversagens eingesetzt (Creutzig & Reinhardt, 2018).

Die Therapie der AML besteht aus einer intensiven Polychemotherapie mit mehreren Zytostatika. Zuerst wird eine intensive Induktionstherapie durchgeführt, eine morphologische Remission, das heißt das Nachlassen von Symptomen kann erst nach 4-8 Wochen Behandlung beurteilt werden. Dies erfordert „weniger als 5 % Blasten im KM, eine Zellularität im KM von über 20 % und mindestens 1000/µl zirkulierende Neutrophile und 80.000/µl Thrombozyten“ (Creutzig & Reinhardt, 2018). Im Anschluss daran folgt die Konsolidierung, also die Erhaltungstherapie beziehungsweise die Intensivierung über einen Zeitraum von 4 bis 6 Monaten. Gegebenenfalls kann eine ZNS-Bestrahlung oder eine allogene Stammzelltransplantation von Nöten sein. Dies ist abhängig von der zuvor erwähnten Risikoabschätzung (Creutzig, Dworzak & Reinhardt, 2019).

Ein Monitoring zum Nachweis der minimalen Resterkrankung (MRD) in der AML wird zwar empfohlen, bietet jedoch im Gegensatz zur akuten lymphoblastischen Leukämie (ALL) kein verbessertes Überleben. Dies liegt vor allem an der Schwierigkeit, geeignete Marker zur Detektion zu finden, da bisher verwendete Marker, aufgrund der diffizilen Molekulargenetik nur für Subgruppen einsetzbar sind (Voso et al., 2019). Denkbar wäre hier die zusätzliche Nutzung der extrazellulären Vesikel, um die MRD-Detektion durch deren Informationen zu sensitivieren.

1.3 Mutationen

Wie in Kapitel 1.2 bereits erwähnt, gibt es in der Diagnostik der AML eine Definition von prognostischen Gruppen aufgrund ihrer genetischen Eigenschaften (siehe Abb. 1). Studien konnten zeigen, dass sowohl die Häufigkeit, als auch die Kombination dieser einzelnen genetischen Veränderungen altersspezifisch sind (Balgobind et al., 2011). Grundsätzlich wird angenommen, dass für die Entstehung der AML 2 Klassen von genetischen Veränderungen interagieren und gleichzeitig vorliegen müssen, die sogenannten Typ-I und Typ-II Aberrationen (Balgobind et al., 2011).

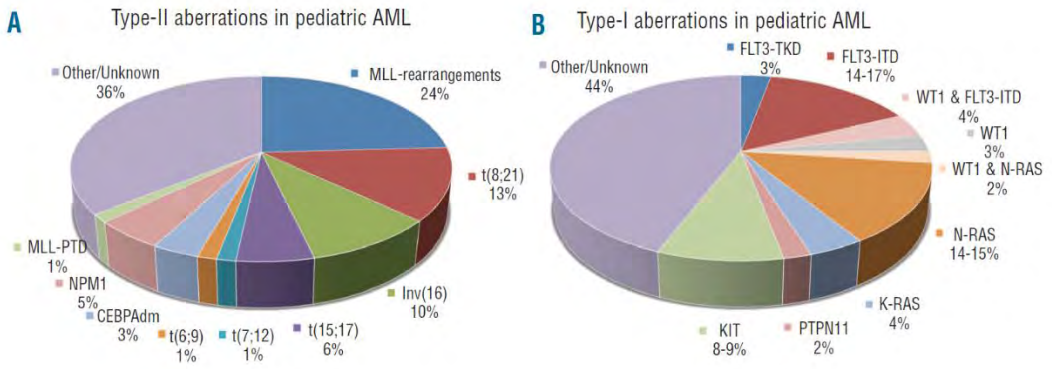

Abbildung 2 **Verteilung der verschiedenen Typ-I und Typ-II Aberrationen in der pädiatrischen AML** (Balgobind et al., 2011).

Die beiden Aberrations-Typen weisen verschiedene Eigenschaften auf, was sich im Ort der Mutation widerspiegelt. Während Typ-I-Aberrationen eine „exzessive, unkontrollierte Proliferation der Leukämiezellen zur Folge haben und sich häufig als Mutationen in den Genen der Signaltransduktionswege wiederfinden, hemmen die Typ-II-Aberrationen die Differenzierung und sind Folge genetischer Veränderungen von Transkriptionsfaktoren, zum Beispiel durch AML-charakteristische Translokationen oder Mutationen in einzelnen Genen“ (Creutzig & Reinhardt, 2018). Abbildung 2 zeigt die Verteilung der einzelnen Mutationen in Bezug auf ihren Aberrationstyp. Trotz vieler Zuordnungen bleibt eine Vielzahl von Aberrationen bislang ungeklärt (Balgobind et al., 2011). Die Testung der Patienten auf die verschiedenen Mutationen ist essenziell für das weitere Vorgehen. So sind durch die Risikogruppen Prognoseschätzungen bezüglich des Therapieansprechens möglich (Creutzig et al., 2016).

Zu den häufigsten Genmutationen gehören CEBPA, NPM1 und FLT3-ITD. CCAAT Enhancer Binding Protein α, oder auch CEBPA ist ein Transkriptionsfaktor, der auf Chromosom 19q13.1 kodiert wird und bei der Vermittlung von zellulärer Differenzierung und Wachstumsstopp eine maßgebliche Rolle spielt (Nerlov, 2007). Die Mutation dieses Proteins ist in 10-15 % der AML-Patienten zu finden und ist oftmals mit einem günstigen Outcome assoziiert (Taskesen et al., 2011). Die zweite vermehrt zu findende Mutation liegt im Nucleophosmin 1 (NPM1), einem Gen für das Protein Nucleophosmin. „Bisher wurden vier Hauptfunktionen von NPM1 beschrieben, darunter eine Rolle bei der Ribosomen-Biogenese (Hingorani, Szebeni, & Olson, 2000),

der Aufrechterhaltung der Genomstabilität (Okuda et al., 2000), der p53-abhängigen Stressreaktion und der Modulation von wachstumsunterdrückenden Signalwegen“ (Colombo, Marine, Danovi, Falini, & Pelicci, 2002). Bei einer Mutation dieses Genes kommt es zu einer 4-Basen-Paar (bp)-Insertion im Exon 12 des NPM1 Gens (Heath et al., 2017). Diese Mutation ist bisher eine der am häufigsten gefundenen in der pädiatrischen AML. Eine weitere oft vertretende Mutation liegt in der Fms-Like Thyrosin Kinase 3 (FLT3). Es handelt sich hierbei um ein Proto-Onkogen, welches an wichtigen Schritten in der Hämatopoese beteiligt ist (Lagunas-Rangel & Chávez-Valencia, 2017). Die zuerst beschriebene und bekannteste Mutation ist die interne Tandem-Duplikation, auch ITD genannt, in den Exonen 14 und 15 (Nakao et al., 1996). Diese liegt oft in Kombination mit anderen Mutationen vor und geht mit einer schlechten Prognose einher (Kiyoi, Kawashima, & Ishikawa, 2020). Eine weitere Form der FLT3 Mutation wäre zum Beispiel die Missense-Punktmutation in Exon 20, auch FLT3-TKD genannt, die jedoch nur eine untergeordnete Rolle spielt (Lagunas-Rangel & Chávez-Valencia, 2017).

1.4 Extrazelluläre Vesikel

Seit mehr als einer Dekade lässt sich ein zunehmendes wissenschaftliches Interesse an extrazellulären Vesikeln (EV) (Skog et al., 2008) verzeichnen.

Es zeigte sich, dass extrazelluläre Vesikel eine Vielzahl anwichtigen Biomoleküle enthalten, dabei unter anderem spezifische Proteine und Lipide sowie funktionelle Nukleinsäuren wie mRNA und microRNA (Deregibus et al., 2007; Valadi et al., 2007). In vergangenen Studien konnte außerdem neben dem Vorkommen von Einzel- auch das von Doppelstrang-DNA bestätigt werden (Thakur et al., 2014). Da EVs viele wichtige Biomoleküle enthalten, die sie auch transferieren können, sind sie durch den Austausch mit unterschiedlichen Zellen in der Lage, biologische Prozesse zu regulieren und das Immunsystem durch die Steuerung von biologischen Signalwegen zu beeinflussen (Yáñez-Mó et al., 2015).

Insbesondere dieses Wissen macht sie zu nützlichen Werkzeugen zum Verständnis der Krebsentstehung sowie zu potenziellen Biomarkern in der Krebsdiagnostik.

Aufgrund ihrer Variabilität in Größe und Funktion sowie Synthese und Inhalt, lassen sich extrazelluläre Vesikel in verschiedene Subtypen einteilen. Die drei Hauptkategorien werden durch Mikrovesikel, Exosomen und apoptotische Körperchen gebildet (Borges, Reis, & Schor, 2013).

Während die Exosomen mit einem Durchmesser von 50-150 nm durch die Exozytose von multivesikulären Endosomen sezerniert werden (Tkach, Kowal, & Théry, 2018), werden die Mikrovesikel (Durchmesser von 100 – 1000 nm) von den Zellen freigesetzt, wo sie sich von der Plasmamembran ihrer ursprünglichen Zelle abschnüren (Choi, Kim, Kim, & Gho, 2015) (siehe Abb. 1). Die Bildung von apoptotischen Körperchen, die die dritte Hauptgruppe der extrazellulären Vesikeln darstellen, erfolgt hingegen während der Apoptose einer Zelle. Diese durchläuft mehrere Stadien, in denen zuletzt der Zerfall des Zellinhalts in membranumschlossene Vesikel erfolgt (Akers, Gonda, Kim, Carter, & Chen, 2013).

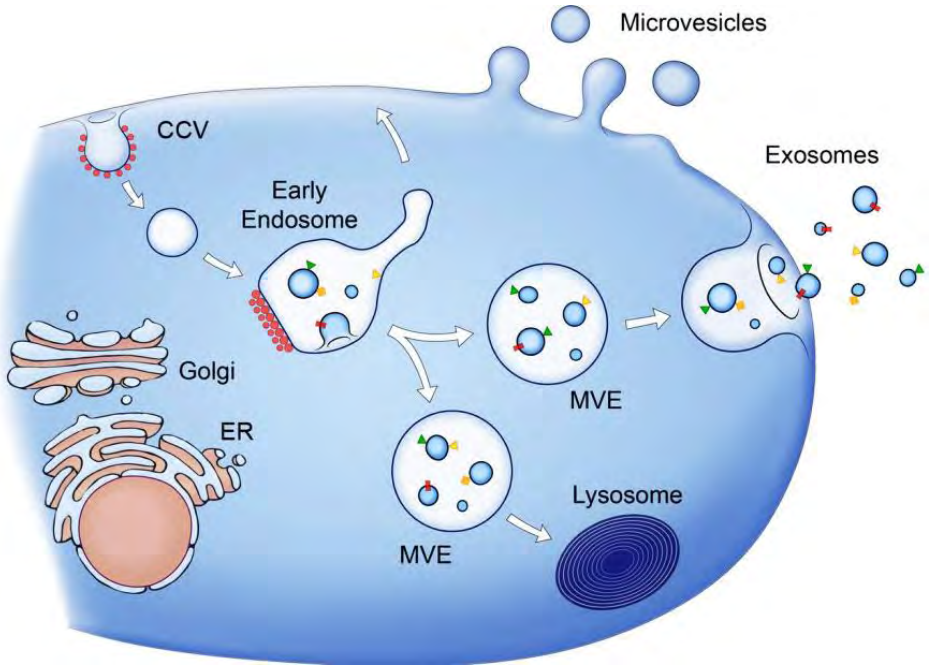

Abbildung 3 Biogenese von extrazellulären Vesikeln - Während Mikrovesikel durch direkte Abschnürung aus der Plasmamembran entstehen, erfolgt die Biogenese von Exosomen intrazellulär durch eine Clathrin-vermittelte Endozytose (clathrin-coated vesicles [CCV]). Hierbei wölbt sich ein Segment der Zellmembran mit Hilfe des Proteins Clathrin nach innen und wird dort abgeschnürt. Das dabei entstandene frühe Endosom (Early Endosome) spaltet sich nun in weitere Vesikel auf, die z.B. mRNA, miRNA, DNA oder Proteine enthalten, und bildet sogenannte Multivesikuläre Körper (Multicellular endosomes [MVE]). Diese intraluminalen Vesikel werden nun entweder durch Fusion der MVEs mit der Plasmamembran als Exosomen in den Extrazellulärraum freigesetzt oder zu den Lysosomen transportiert. Die hier dargestellten Pfeile stellen vorgeschlagene Richtungen des Protein- und Lipidtransports dar (Raposo und Stoorvogel 2013).

Aufgrund der einfachen Zugänglichkeit, bieten EVs in der klinischen Anwendung große Vorteile. Bislang konnten sie aus verschiedensten Körperflüssigkeiten, wie Urin, Fruchtwasser, malignem Aszites, bronchoalveolärer Lavageflüssigkeit, Synovialflüssigkeit, Muttermilch, Speichel und Blut, sowie aus den Kulturmedien einer Vielzahl von Zelltypen isoliert werden (Simpson, Lim, Moritz, & Mathivanan, 2009), was ihre große Spannbreite für mögliche diagnostische Assays verdeutlicht.
Eine Teilnahme an der Antigenpräsentation durch B-Lymphozyten, eine Immunsupression beispielsweise bei pathophysiologischen Prozessen oder maligner Entartungen (z.B. Metastasierung) sowie die Verhinderung der Proliferation und Aktivierung von Effektor-T-Zellen sind nur einige Beispiele für nachgewiesene Funktionen der Extrazellulären Vesikel (Batista & Melo, 2019; Clayton et al., 2008; Raposo & Stoorvogel, 2013).
Eine Ursache der Tumorentwicklung ist die genetische Instabilität der Krebszellen. In dieser Phase entlassen sie eine große Menge an EVs, welche zwar auch von gesunden Zellen freigesetzt werden, jedoch nicht in dieser Vielzahl (Bach, Hong, Park, & Lee, 2017). Aufgrund ihrer vielfältigen Funktionen ist es den EVs sogar möglich, die Tumorproliferation und die Tumortransformation zu induzieren und zudem das Absterben von Krebszellen zu hemmen (Batista & Melo, 2019).
Darüber hinaus ist es bereits gelungen, aus EVs gewonnene tumorspezifische mRNA aus dem Serum und Gewebe von Glioblastom-Patienten zu isolieren, die den Mutationsstatus von EGFRvIII widerspiegelt (Skog et al., 2008).

In dieser Studie wurde ein ähnlicher Ansatz des Mutationsstatus der aus den EVs gewonnen DNA und RNA verfolgt.
Es konnten schon zahlreiche Funktionen der Extrazellulären Vesikel untersucht werden. Die genaue interzelluläre Kommunikation oder in welcher Absicht die Vesikel genau aus den Zellen entlassen werden, ist bislang jedoch noch nicht hinreichend geklärt.

2. Ziel der Arbeit

Die vorliegende Arbeit konzentriert sich auf zwei wesentliche Aspekte: zum einen auf die Gewinnung von genetischem Material, in Form von DNA und RNA, aus den extrazellulären Vesikeln. Hierfür wurden 166 Plasmaproben von 45 Patienten mit bekannter AML aus der Biobank der Kinderklinik III der Universitätsklinik Essen aufgearbeitet, deren DNA und RNA wurde extrahiert und anschließend quantifiziert.

Zum anderen wurde mit Assays der derzeit durchgeführten klinischen Diagnostik versucht, Mutationsanalysen mit der DNA und RNA aus extrazellulären Vesikeln ausgewählter, spezifischer AML-Zelllinien zu etablieren.

Nach erfolgreicher Testung auf zellulärer Ebene folgten die Analysen der bereits aufgearbeiteten Patientenproben. Diese wurden, wie auch die Zelllinien, sorgfältig nach ihren Mutationen ausgesucht.

Ziel dieser Arbeit ist es, zu evaluieren, inwieweit die klinische Verwendung dieser Methode, im Vergleich zu der derzeit durchgeführten genomischen DNA-Analyse, zu einer exakteren Diagnosestellung beitragen kann, beziehungsweise ob die Verwendung von extrazellulären Vesikeln im klinischen Alltag ergänzend zum Beispiel in Bezug auf das MRD-Monitoring von Nutzen sein kann.

3. Ergebnisse

3.1 Detection of AML-specific mutations in pediatric patient plasma using extracellular vesicle–derived RNA.

Annals of Hematology (2019) 98:595–603
https://doi.org/10.1007/s00277-019-03608-y

ORIGINAL ARTICLE

Detection of AML-specific mutations in pediatric patient plasma using extracellular vesicle–derived RNA

Fabienne Kunz[1] · Evangelia Kontopoulou[1] · Katarina Reinhardt[1] · Maren Soldierer[1] · Sarah Strachan[1] · Dirk Reinhardt[1] · Basant Kumar Thakur[1]

Received: 23 November 2018 / Accepted: 4 January 2019 / Published online: 23 January 2019

Abstract

Despite high remission rates, almost 25% of patients with AML will suffer relapse 3–5 years after diagnosis. Therefore, in addition to existing diagnostic and MRD detection tools, there is still a need for the development of novel approaches that can provide information on the state of the disease. Extracellular vesicles (EVs), containing genetic material reflecting the status of the parental cell, have gained interest in recent years as potential diagnostic biomarkers in cancer. Therefore, isolation and characterization of blood and bone marrow plasma-derived EVs from pediatric AML patients could be an additional approach in AML diagnostics and disease monitoring. In this study, we attempt to establish a plasma EV-RNA-based method to detect leukemia-specific FLT3-ITD and NPM1 mutations using established leukemia cell lines and primary pediatric AML plasma samples. We were successfully able to detect FLT3-ITD and NPM1 mutations in the EV-RNA using GeneScan-based fragment-length analysis and real-time PCR assays, respectively, in samples before therapy. This was corresponding to the gDNA mutational analysis from leukemic blasts, and supports the potential of using EV-RNA as a diagnostic biomarker in pediatric AML.

Keywords Extracellular vesicles · RNA · Pediatric AML · Biomarker

Introduction

Acute myeloid leukemia (AML) is a very heterogeneous hematological cancer and is the second most common form of leukemia in children [1]. Although there is a high remission rate for AML patients (up to 80%), relapse continues to be the most common cause of death in AML [2, 3]. One of the major challenges in predicting relapse in AML lies in the acquisition of novel secondary mutations in the primary leukemic cells during therapy [1, 4]. Additionally, there is lack of an effective uniform molecular biomarker which can monitor clonal evolution to predict minimal residual disease and relapse [2, 3, 5]. Although cellular analysis of blasts can be effective for diagnosis, the presence of them in the blood can reflect that the disease has already reached an advanced level; therefore, there is a strong need for an alternative diagnostic tool which can predict relapse at an earlier time point.

Extracellular vesicles (EVs) have recently gained interest in the field of cancer due to their novel roles as biomarkers and cell to cell mediators in metastasis and relapse [6, 7]. EVs are a mixed group of membrane-bound vesicles, with exosomes and microvesicles being the two main subtypes of interest in research [8–10]. They are produced by both healthy and cancerous cells and can be found in several body fluids, like blood, urine, or saliva, from where they can be easily isolated and analyzed using a simple liquid biopsy approach [6]. Additionally, it has been shown that the nucleic acids found within EVs can potentially mirror the mutational status of the parental cell from which the EVs originate [6, 11], making them potential candidates for the development of diagnostic tools that could be utilized in a clinical setting.

Furthermore, several other working groups have previously demonstrated that EVs and the RNA they contain have

Fabienne Kunz and Evangelia Kontopoulou contributed equally to this work.

Electronic supplementary material The online version of this article (https://doi.org/10.1007/s00277-019-03608-y) contains supplementary material, which is available to authorized users.

✉ Basant Kumar Thakur
Basant-Kumar.Thakur@uk-essen.de

[1] Department of Pediatric Hematology and Oncology, University Hospital Essen, Hufelandstraße 55, D-45147 Essen, Germany

several characteristics, which could make them ideal biomarkers for the AML disease state. For example, earlier studies have claimed that cancerous cells produce more EVs than healthy cells [6, 12], which has also been observed in the AML disease state, with AML patients having higher numbers of EVs in circulation than healthy controls [13–15]. It has also been shown that the contents of EVs from AML cells can change depending on the disease stage [13], including the upregulation of several miRNAs that are relevant to AML prognosis and relapse [13, 16]. This is further supported by the previous work of Hornick et al. (2015) who showed that EV miRNA could be used to detect leukemic relapse in a mouse model [2, 5]. Furthermore, Huan et al. (2013) have previously shown that it is possible to detect AML-specific mRNA transcripts in EVs from conditioned media of cultured primary leukemia cells and AML cell lines [17] and, in addition, Hong et al. (2014) have previously shown that the level of TGF-β1 protein in EVs can be correlated to the status of therapy in AML [18]. All of these findings further support the idea of using EVs and their RNA content for the detection and monitoring of AML [2, 5, 17, 18].

In this study, for the first time, EV-RNA from primary pediatric patient plasma was investigated for its diagnostic value by attempting to detect AML-specific mutations in the EV-RNA at time points of diagnosis and during treatment. The plasma EV-based method to detect leukemia cell–specific information could potentially provide complimentary data on the stage of leukemia, disease progression, and response to therapy. In future, this could offer an alternative or additional tool to the classical bone marrow puncture for the detection and prediction of pediatric AML.

Material and methods

Ultracentrifugation of patient samples

Seventy-three plasma samples from 16 patients with childhood AML were obtained from the biobank of the Children's Hospital of Essen. Plasma from patients was obtained in varying volumes; therefore, before performing differential centrifugation and ultracentrifugation steps for EV isolation, the sample volume was adjusted to 2 ml by adding PBS, as required. A normal centrifugation for 20 min at 3000×*g* at 10 °C had been previously performed. The supernatant was collected in new tubes and centrifuged at 12,000×*g* for 20 min at 10 °C. The supernatant was transferred into 4-ml ultracentrifuge tubes (Beckman Coulter No. 355645) and samples were balanced with a maximum difference of 0.01 g before performing ultracentrifugation. Samples were ultracentrifuged using a fixed angle rotor Ti 50.4 (Beckman Coulter) at 100,000×*g* for 70 min at 10 °C. The supernatants were discarded and the pellet containing EVs was washed by resuspending in 2 ml of PBS and ultracentrifuged at 100,000×*g* for 70 min at 10 °C. After discarding the supernatant, the final EV pellet was resuspended in 250 μl of PBS. From the obtained EV pellet, 20 μl was used as aliquots for further analysis.

The same protocol was used for the isolation of EVs from conditioned media of leukemia cell lines, with the only differences being the volume and the rotor (Ti 45, Beckman Coulter) which were used. The conditioned media from each flask of each leukemia cell line were transferred into one 94-ml ultracentrifuge tube (Beckman Coulter No. 355628) and was ultracentrifuged to obtain purified EVs. The final EV pellets were resuspended in 250 μl of PBS, transferred into microcentrifuge tubes, and frozen at − 80 °C.

Cell culture

Leukemia cell line MV4-11 (acute monocytic leukemia) was cultured in RPMI-1640 media (Gibco No. 21875-034) with 10% FBS (Biowest, No. S1860-500) and 1% Pen-Strep (Gibco No. 15140-122), and OCI-AML3 (acute myeloid leukemia) was cultured in MEM Alpha media (Gibco No. 12561056) with 20% FBS and 1% Pen-Strep . When enough cells were obtained, the cells from each flask were centrifuged at 300×*g* for 5 min and the pellet was resuspended in 1 ml of RPMI-1640 media or MEM Alpha media with 10% or 20% EV-depleted FBS and 1% Pen-Strep. Next, 3.5×10^6 cells were then transferred into 12 T175 flasks (Cell star No. 660175) with 24 ml of EV-depleted media. This assured that the supernatant would contain only EVs released from the cells. After 48 h, an additional 25 ml of this media was added to the flasks and left for an additional 24 h. This supernatant was collected and used in ultracentrifugation to obtain EVs for further analysis.

ZetaView analysis—nanoparticle tracking analysis

Nanoparticle tracking analysis (NTA-ZetaView, Particle Metrix GmbH) was performed to characterize EVs according to the recommendations of the International Society of Extracellular Vesicles (ISEV). Fresh standards were prepared using "100 nm standard beads." First, 10 μl of standard was added to 10 ml of H_20 (1:1000). Then, 188 μl of the 1:1000 solution was transferred into another falcon which contained 50 ml H_20 (1:266,000). All the settings were adjusted using the standard beads, and the concentration of the samples was adjusted using DPBS in order to obtain the number and the size of the particles that did not exert the minimum and maximum values of the settings. The final volume of diluted samples loaded onto the ZetaView was 1 ml. At least two washes of 10 ml DPBS were performed to clean the sample loading platform of the ZetaView between the measurements of each sample. The zeta potential, number of EVs, and size histograms were generated by built-in software of the ZetaView instrument.

RNA isolation and quantification

The RNA isolation was performed using the NucleoSpin® RNA XS (Macherey-Nagel No. 740902.50) according to the manufacturer's instructions. Briefly, 200 μl of Buffer RA1 and 4 μl of TCEP were added to each 50 μl isolated EV sample and vortexed vigorously. Next, 300 μl of 70% ethanol was added to the homogenized lysate and mixed by pipetting. Each sample was loaded into a Nucleospin RNA XS column and centrifuged at 11,000×*g* for 30 s. Then, 100 μl MDB (Membrane Desalting Buffer) was added and centrifuged at 11,000×*g* for 30 s. Next, 25 μl of rDNase reaction mixture was applied directly onto the center of the column and incubated at RT for 15 min. A wash step was performed by adding 100 μl of Buffer RA2 to the column, followed by a centrifugation of 11,000×*g* for 30 s. Two extra washing steps took place by applying 400 μl and 200 μl of Buffer RA3 and centrifuged at 11,000×*g* for 30 s and 2 min, respectively. RNA was eluted in 45 μl of RNase-free H_2O. The RNA concentration was quantified using the RNA Quantifluor (Promega No. E3310) system according to the instructions of the manufacturer.

cDNA synthesis

The isolated RNA was transcribed into cDNA using a Transcriptor First Strand DNA Synthesis Kit (Roche No. 04897030001). Briefly, 2 μl of the provided random hexamer primer and 11 μl of RNA were transferred into a 0.2-ml Eppendorf tube. The samples were heated for 10 min at 65 °C and then cooled on ice. Next, 7 μl of a master mix consisting of the provided reverse transcriptase reaction buffer, protector RNase inhibitor, deoxynucleotide mix, and reverse transcriptase was added to the RNA/oligonucleotide primer solution, to a final volume of 20 μl. For the cDNA synthesis, samples were heated at 25 °C for 10 min, followed by 55 °C for 30 min and 85 °C for 5 min in a C1000 Thermal Cycler (Bio-Rad).

GeneScan-based fragment-length analysis

For the detection of the FLT3-ITD mutation, GeneScan-based fragment-length analysis was performed. First, PCR was performed with the following primers: FLT3-ITD forward 5′-GTAAAACGACGGCCAGGCAATTTAGGTATGAAAGCCAGC-3′ and reverse 5′-CAGGAAACAGCTATGACCTTTCAGCATTTTGACGGCAACC-3′ (Eurofins). Next, 20.5 μl of the Master Mix (which contained 12.5 μl ALL in Hot Start Taq 2× MM (HighQu), 6 μl H_2O, and 1 μl of the forward and reverse primers with a concentration of 10 pmol/μl) was added together with 4.5 μl of the sample into a 0.5-ml Eppendorf tube. The same mixture without the sample was prepared as control. For amplification, samples were heated at 95 °C for 2 min, followed by 40 cycles of 95 °C for 15 sec, 59 °C for 15 sec, and 72 °C for 15 sec. PCR products were diluted (1:80) in H_2O. Next, 1 μl of diluted PCR products was mixed with 10 μl HiDi Formamid (Thermo Fisher) and 0.3 μl GeneScan-based fragment-length analysis 600 LIZ Size Standard v 2.0 (Thermo Fisher). PCR products were denatured for 5 min at 95 °C. GeneScan-based fragment-length analysis was performed using the 3500 genetic analyzer and data were analyzed with GeneMapper Software 5 (Thermo Fisher).

RT-PCR

Qualitative and quantitative detection of the mutated NPM1 gene (OMIM No. 1640401) was done by RT-PCR. The protocol has been optimized from the standard operational procedure (SOP), which was developed by the European molecular net. The following primers were used: NPM1_forward: 5′-CAAAGTGGAAGCCAAATTCATC-3′; NPM1_reverse: 5′-CCTCCACTGCCAGACAGA-3′; probe: 5′-TAGCCTCTTGGTCAG-TCATCCGGAAGCA [BHQ1]-3′ (Eurofins). The ABL2 gene (OMIM 164690) was used as a housekeeping gene: ABL_forward: 5′-GGGTCCACACTGCAATGTTT-3′; ABL_reverse: 5′-CCAACGAGCGGCTTCAC-3′; probe: 5′-TCAGATGCTACTGGCCGCTGAAGG [BHQ1]-3′. Probes were synthesized by Eurofins (Ebersberg). All samples were performed in triplicate, including controls (ABL2 and H_2O). In each well of a 96-well plate, 17 μl of the Master Mix, 12.5 μl of TaqMan Universal Master Mix (Thermo Fisher), 2 μl of H_2O, and 2.5 μl of 10× primer mix were added. This primer mix contained 3 μM of the primer (forward/reverse) and 2 μM of the probe (FAM and H_2O). Next, 3 μl of cDNA was added to each well, which was then sealed with optical caps. The plate was briefly spun down and loaded onto the StepOne™ Real-Time PCR System (Thermo Fisher).

Transmission electron microscopy

Transmission electron microscopy (TEM) was performed at the Imaging Center Essen (IMCES) for visualization of the EVs. Firstly, mesh copper grids coated with formvar (PLANO No. SF162) were made hydrophilic by exposing them to glow discharging for 1.5 min (PELCO easiGlow™). Afterwards, 3 μl of EV sample was added to the grids, which were then negatively stained for 1 min with 3 μl of 1% *v/v* uranyl acetate. The excess liquid was removed and the grids were dried for 15 min and finally observed under a JEOL 1400+ TEM Crossbeam at 120 kV (JEOL).

Results

EV isolation from leukemia cell lines

Two different cell lines, OCI-AML3 carrying a NPM1 mutation and MV4-11 carrying a FLT3-ITD mutation, were cultured for 72 h in EV-depleted growth medium. EVs were extracted from conditioned medium using differential centrifugation followed by ultracentrifugation steps. The characterization of the EVs (Supplementary Table S1), to estimate their number and their average diameter, was performed by NTA. Average particle size of both cell lines was in the range of 30–160 nm (Fig. 1a, b, Supplementary Fig. 1a). Transmission electron microscopy was performed to visualize EVs in order to further confirm their presence and size (Fig. 1b–e). These results confirmed the successful isolation of EVs based on the expected EV size range (30–150 nm), allowing the continuation of further molecular analyses.

EV-derived RNA from leukemia cell lines reflects the genomic mutational status

To firstly check whether it was possible to detect the mutations in each cell line and to compare the mutational status of the cell lines with their EVs, RNA was extracted from the EVs (Fig. 2a) and cells of both cell lines. The RNA was transcribed into cDNA and the mutational detection was performed by two different assays. RT-PCR was used for the detection of the NPM1 mutation, while GeneScan-based fragment-length analysis was performed for the FLT3-ITD mutation. The NPM1 mutation was detectable in RNA extracted from both cells and EVs (Fig. 2b, Supplementary Fig. 1b and c). The FLT3-ITD mutation was also

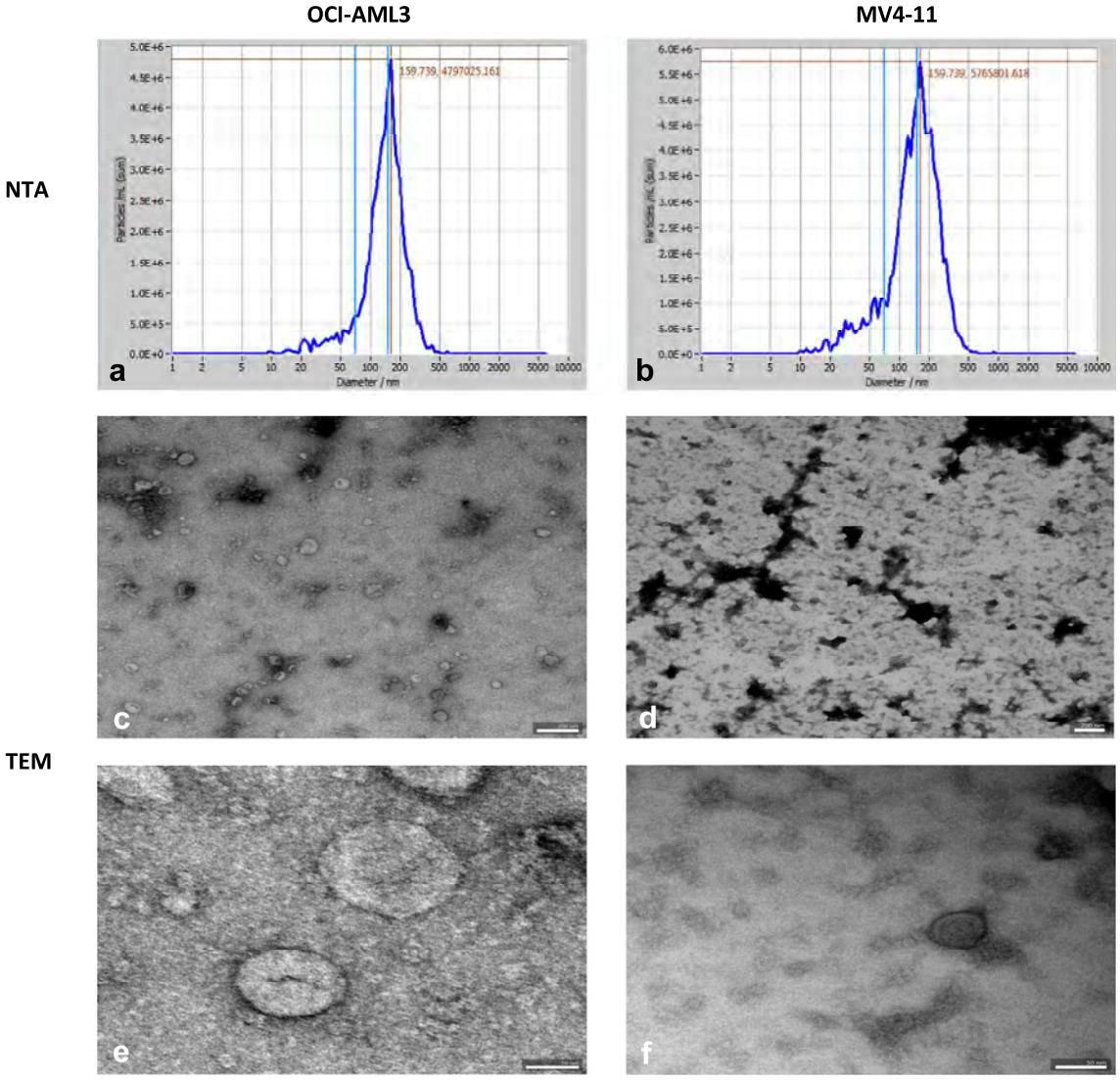

Fig. 1 **a**, **b** Particle diameter size and number of particles in leukemia cell line supernatant, as measured by nanoparticle tracking analysis (NTA). The size distribution is in the range of extracellular vesicles (30–160 nm). **c**–**f** Transmission electron microscopy of uranyl acetate–stained EVs from leukemia cell line supernatant. Scale bar 200 nm

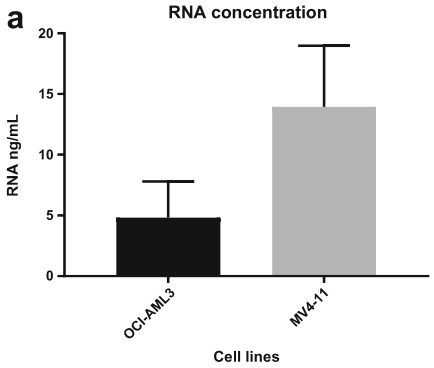

b

Cell line	NPM1	FLT3-ITD
OCI-AML3 EVs	+	-
OCI-AML3 cells	+	-
MV4-11 EVs	-	+
MV4-11 cells	-	+

Fig. 2 **a** Comparison of RNA concentration, extracted from EVs of two leukemia cell lines. **b** Results of RNA mutational analyses. RT-PCR analyses for NPM1 mutation were performed to compare the sensitivity of mutational detection in RNA that was extracted from EVs of one cell line (OCI-AML3) with the RNA extracted from the cells of both cell lines. For the assay, maximum volume of 3 μl was used from each sample. The NPM1 AML-specific mutations were not present in negative control cell line (MV4-11), however, the OCI-AML3 cell RNA and EV-RNA were both positive for the NPM1 mutation. GeneScan-based fragment-length analyses for detection of FLT3-ITD mutation in MV4-11 cell RNA and EV RNA were also performed. Negative control OCI-AML3 cell RNA was negative for the FLT3-ITD mutation and MV4-11 cell RNA and EV-RNA were positive for the FLT3-ITD mutation

detectable in both cases and, interestingly, was higher expressed in EVs in comparison with cell-derived RNA (Fig. 2b).

EV isolation from pediatric AML patient samples

To further investigate if the mutational status of a patient can be detected from plasma-derived EVs, EVs were isolated from AML patient samples by performing differential centrifugation followed by ultracentrifugation steps. The plasma-derived EVs were analyzed for their number and size by NTA, and the number of EVs obtained from samples before and after treatment was compared (Supplementary Tables S2 and S3). The average particle size was in the range of 30–160 nm (Fig. 3a–d) and TEM was performed to confirm the NTA results (Fig. 3e–h). In patients carrying the NPM1 mutation, as well as in patients with a combined mutation (NPM1 and FLT3-ITD), the number of particles was always lower in the after-treatment EV samples than in the before-treatment EV samples (Fig. 3i). In contrast, the patient group with the FLT3-ITD mutation only revealed a higher particle concentration in the after-treatment samples compared with the before-treatment samples (Fig. 3i). A decrease in the number of EVs after treatment would be expected as this would correlate with the decrease in cancerous cells, as well as with the reduced leukemic blast cells after treatment (Supplementary Table S2). The number of the EVs in the before-treatment samples between the different mutational groups is statistically significantly different revealing a correlation between the number of the released EVs and the mutational group that they belong to.

EV samples from pediatric AML patients contain RNA

To establish the EV-RNA as a potential tool for the detection of AML mutations in patient samples, RNA was extracted from the plasma-derived EVs of 16 AML patients. The EV-RNA concentration was measured by RNA QuantiFluor (Supplementary Table S3). The amount of obtained EV-derived RNA was higher in the before-treatment samples than in the after-treatment samples in AML patients with the NPM1 mutation only or with a combined mutation (Fig. 4a). In contrast, the EV-derived RNA from patients with the FLT3-ITD mutation only showed higher concentrations after treatment in comparison with the before-treatment samples (Fig. 4a). This mirrors the results of the NTA, which indicate the same trend in EV number.

EV-derived RNA reflects the patient mutational status

Next, we investigated whether the EV-RNA of the AML patients reflected their mutational status. EV-RNA from patients carrying a NPM1 mutation was obtained, transcribed into cDNA, and analyzed for the mutational status by RT-PCR. In seven AML patients, identical mutations were detected in the EV-RNA of the initial samples before therapy and in the primary leukemic blasts. In two patients, it was not possible to detect the mutation in the initial sample at all (Fig. 4b, Supplementary Table S4). In all patient samples after therapy, the initial AML-specific mutation was no longer detectable (Fig. 4b, Supplementary Table S4). GeneScan-based fragment-length analysis was performed for the mutational analysis of nine AML patients with a FLT3-ITD mutation. For this purpose, EV-derived RNA was extracted and transcribed into cDNA and GeneScan-based fragment-length analysis was performed. The mutation was detectable in all of the initial samples before treatment (Fig. 5a–d), but it was not possible to detect it in the after-treatment samples of each patient (Supplementary Table 4). This lack of mutational detection for both mutations in all after-treatment patient samples was not always in correlation to the results of the gDNA analysis that is routinely performed in our diagnostic AML lab after every treatment.

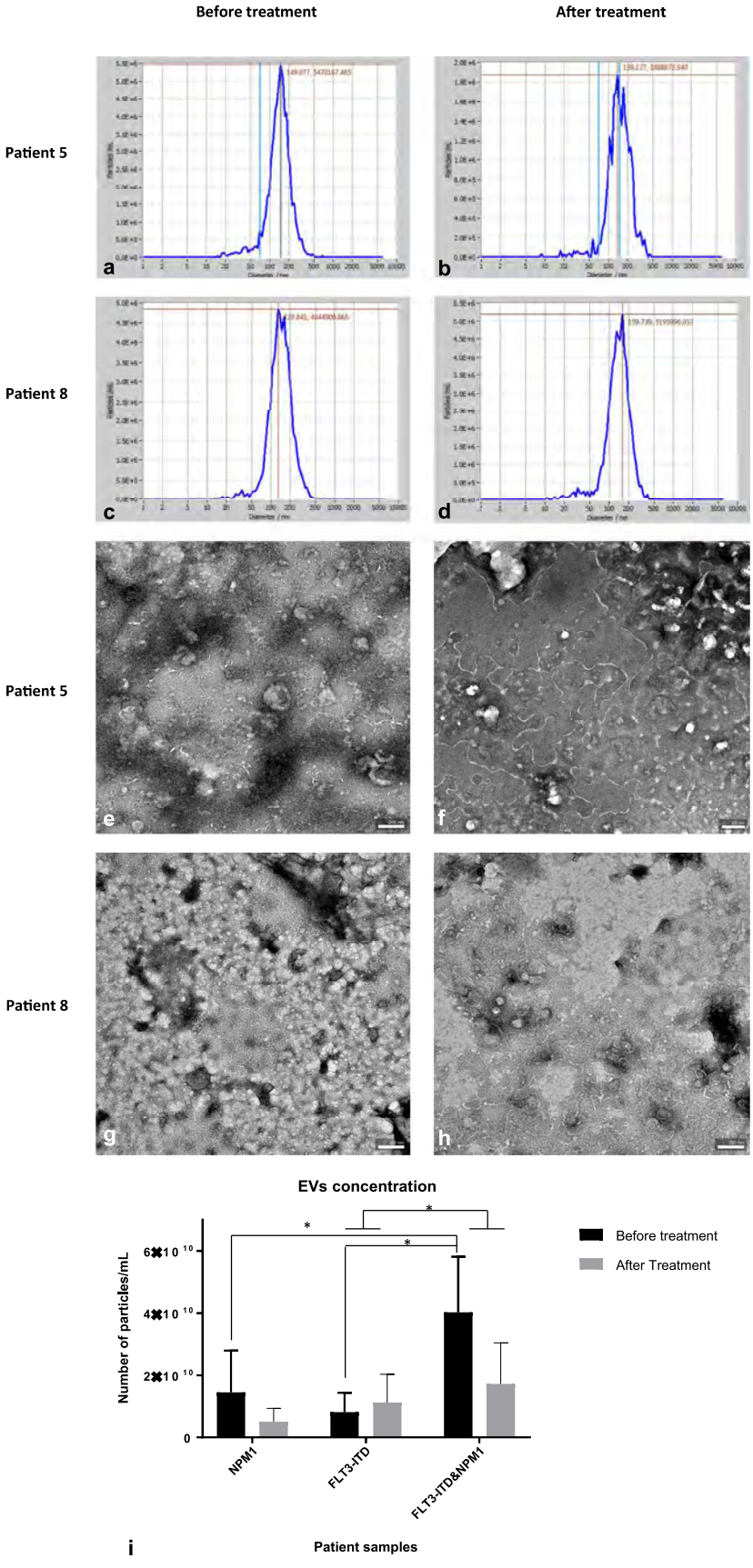

Fig. 3 **a**–**d** Particle diameter size and number of particles per mL of plasma from two AML patients before and after treatment, as measured by nanoparticle tracking analysis (NTA). The size distribution is in the range of extracellular vesicles (30–160 nm). **e**–**h** Transmission electron microscopy of uranyl acetate–stained EVs from patient plasma samples before and after treatment. Scale bar 200 nm. **i** Comparison of EVs concentration in before- and after-treatment samples from 16 AML patients, as measured by NTA analysis. Higher concentration of EVs in before-treatment samples was observed in patients with NPM1 mutation only and with combined mutations than those with a FLT3-ITD mutation only. The difference in EV concentration between patients with a FLT3-ITD mutation only and patients with FLT3-ITD and NPM1 combined mutations was statistically significant ($p = 0.0145$). In addition, EV concentration in before-treatment samples of patients carrying both mutations was statistically significantly higher than in the NPM1 only group ($p = 0.0468$) and the FLT3-ITD only group ($p = 0.0168$)

Discussion

Despite the recent advances in the treatment and diagnosis of AML, which is reflected by high remission rates, many patients are still suffering from relapse—the biggest cause of death in AML [2, 3]. This highlights the ongoing need for the development of a more sensitive approach with the ability to detect and monitor this disease more effectively. Simultaneously, this approach should encompass the advantage of reducing pain and inconvenience for the patients caused by the current standard bone marrow puncture–based diagnostic methods. In the current study, we attempted to take the first steps towards the development of a tool that would fulfill these criteria by evaluating the diagnostic potential of plasma-derived EV-RNA in pediatric AML.

Here, using both established leukemia cell lines and AML pediatric patient samples ($n = 16$), we have demonstrated the biomarker potential of EV-derived RNA in AML. Using cell line–conditioned media, we successfully established that it was possible to isolate EVs, extract RNA, and detect AML-specific mutations, NPM1 and FLT3-ITD, using RT-PCR and GeneScan-based fragment-length analysis methods, respectfully. These positive results reflected that our proposed isolation and detection methods were valid and functional at the cell line level. Subsequently, using the same methods, RNA was isolated from EVs of pediatric patient plasma ($n = 16$), before and after treatment, and analyzed for its biomarker potential. In 14 out of the 16 AML patient samples at the stage of primary diagnosis, it was possible to detect NPM1 or FLT3-ITD mutations which reflected the known gDNA information of the samples. These initial results showed that our approach was sensitive enough to detect AML-specific mutations from a source of plasma containing heterogeneous populations of EVs, highlighting that the approach does indeed have

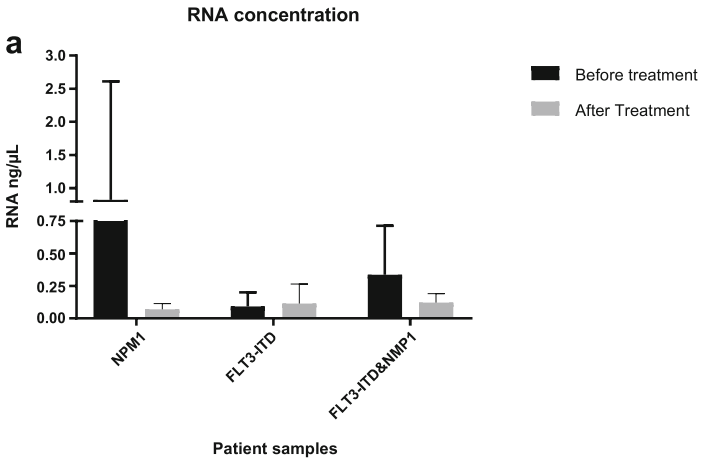

b

Patient	Mutation	Primary leukemia blasts	EV RNA Before treatment	EV RNA After treatment in different blocks						
P3	NPM1	+	+	-*	-*	-*	-*			
P4	NPM1	+	+	-	-	-	-	-		
P5	NPM1	+	+	-	-					
P7	NPM1	+	+	-*	-*	-*	-*	-*	-	-
P9	NPM1	+	+	n.a						
P10	NPM1	+	+	-*	-*	-*	-*			
P14	NPM1	+	+	-	-*					
P15	NPM1	+	n.a	-*	-*					
P16	NPM1	+	n.a	-*	-*					

Fig. 4 **a** Comparison of RNA concentration, extracted from EV fractions of 16 AML patients, prior and post treatment. **b** RT-PCR for NPM1 mutation was performed to establish the sensitivity of mutational detection in RNA that was extracted from EVs of patients, and compared with the already existing patient mutational status information of the primary leukemia database in the AML-BFM lab. Sixteen patient samples before and after treatment were used for analysis. A maximum volume of 3 µl from each sample was used. AML-specific mutations were not present in post-treatment samples.*Low-quality sequencing data. -*No mutation detected but low-quality sequencing data

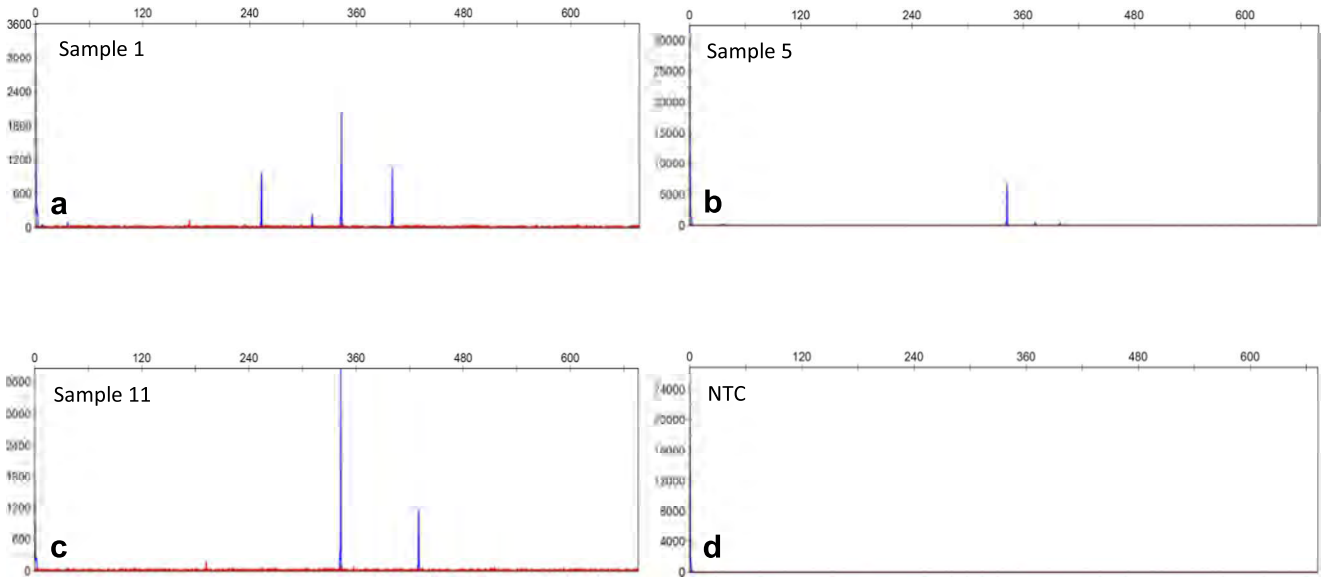

Fig. 5 **a**–**d** GeneScan-based fragment-length analysis of FLT3-ITD mutation was performed to establish the sensitivity of mutational detection in RNA that was extracted from EVs of patient samples, and compared with the already existing patient mutational status information of the primary leukemia database in the AML-BFM lab. Sixteen patient samples before and after treatment were used for analysis. 50 ng/μl or a maximum volume of 10.5 μl from each sample was used. Samples **a**, **b**, and **c** are before-treatment samples that show the FLT3-ITD mutation (size ~ 372). Sample **d** is the negative control. AML-specific mutations were not present in post-treatment samples (data not shown)

diagnostic biomarker potential. In addition, the number of EVs and the consequent amounts of RNA appeared to be influenced by the mutational background of the patients. As previous studies have shown that AML patients have more EVs than healthy controls [13–15], this was an interesting observation, which once established in a larger patient cohort study may have additional diagnostic utility.

The proposed approach, with the current sensitivity, does in fact have its limitations. Although it was successful at detecting mutations in almost all patients at initial diagnosis, it was not always possible to detect mutations after treatment when using this method. These are issues that must be addressed, as sensitivity is of utmost importance when designing diagnostic detection methods. These results could be attributed to the lower amount of RNA that was recovered from these samples; perhaps due to a reduction in EV production by mutation-containing cells or a reduction of the cells themselves. Alternatively, they could also be related to the EV heterogeneity of the plasma. Like all new approaches, this method also requires a period of optimization before its implementation as a clinically routine method can be considered. Therefore, in future, this study should be repeated using a larger cohort of patients and with an enhanced EV isolation method, capable of specifically sorting for AML-derived EVs.

Despite the discussed points of needed improvements in sensitivity, the advantage of this method over current diagnostic methods is clear, in terms of patient welfare. A liquid biopsy approach could indeed be a valuable diagnostic tool, offering a fast, pain-free, and hassle-free alternative to current painful bone marrow biopsies. Being able to diagnose or monitor a leukemic disease simply by drawing blood and isolating EVs instead of having to undergo a bone marrow puncture procedure would be much more convenient and less stressful for pediatric patients. In conclusion, our approach to establish an EV-RNA-based diagnostic platform provides valuable information that could be potentially useful in the future diagnosis and treatment of AML. This preliminary study definitely provides a starting point for the use of EV-RNA as a disease biomarker in AML and, once the sensitivity is optimized and the study is recapitulated in larger cohorts of patients, will open the door to many possible avenues of future research on this topic.

Authors' contributions Conception and design: BKT, FK, EK; collection and assembly of data: FK, EK, KR, MS; data analysis and interpretation: BKT, FK, EK; drafting of manuscript: BKT, FK, EK, SS; manuscript writing: BKT, FK, EK, SS; final approval of manuscript: all co-authors.

Funding This study was supported by the José Carreras Leukemia Foundation promotion grant 04 PSG/2017 awarded to Fabienne Kunz and Stiftung Universitätsmedizin Essen grant on cancer exosome research awarded to Dr. Basant Kumar Thakur.

Compliance with ethical standards

Conflict of interest The authors declare that they have no conflict of interest.

Informed consent Informed consent was obtained from all individual participants (or their parents) included in the study. Each patient consented following institutional review board approval AML-BFM 2004 (3VCreutzig1).

Ethical approval All procedures performed in studies involving human participants were in accordance with the ethical standards of the institutional and/or national research committee and with the 1964 Helsinki declaration and its later amendments or comparable ethical standards.

Statement on the welfare of animals This article does not contain any studies with animals performed by any of the authors.

Publisher's Note Springer Nature remains neutral with regard to jurisdictional claims in published maps and institutional affiliations.

References

1. Trino S, Lamorte D, Caivano A, Laurenzana I, Tagliaferri D, Falco G, Del Vecchio L, Musto P, and De Luca L (2018) MicroRNAs as new biomarkers for diagnosis and prognosis, and as potential therapeutic targets in acute myeloid leukemia, Int J Mol Sci 19(2):460
2. Hornick NI, Huan J, Doron B, Goloviznina NA, Lapidus J, Chang BH, Kurre P (2015) Serum exosome microRNA as a minimally-invasive early biomarker of AML. Sci Rep 5:11295
3. Paietta E Minimal residual disease in acute myeloid leukemia: coming of age. Hematol Am Soc Hematol Educ Program 2012, 2012: 35–42
4. Grove CS, Vassiliou GS (2014) Acute myeloid leukaemia: a paradigm for the clonal evolution of cancer? Dis Model Mech 7:941–951
5. Boyiadzis M, Whiteside TL (2016) Plasma-derived exosomes in acute myeloid leukemia for detection of minimal residual disease: are we ready? Expert Rev Mol Diagn 16:623–629
6. Becker A, Thakur BK, Weiss JM, Kim HS, Peinado H, Lyden D (2016) Extracellular vesicles in cancer: cell-to-cell mediators of metastasis. Cancer Cell 30:836–848
7. Keller S, Ridinger J, Rupp AK, Janssen JW, Altevogt P (2011) Body fluid derived exosomes as a novel template for clinical diagnostics. J Transl Med 9:86
8. Gould SJ, and Raposo G (2013) As we wait: coping with an imperfect nomenclature for extracellular vesicles, J Extracell Vesicles 2:20389
9. Raposo G, Stoorvogel W (2013) Extracellular vesicles: exosomes, microvesicles, and friends. J Cell Biol 200:373–383
10. Abels ER, Breakefield XO (2016) Introduction to extracellular vesicles: biogenesis, RNA cargo selection, content, release, and uptake. Cell Mol Neurobiol 36:301–312
11. Thakur BK, Zhang H, Becker A, Matei I, Huang Y, Costa-Silva B, Zheng Y, Hoshino A, Brazier H, Xiang J, Williams C, Rodriguez-Barrueco R, Silva JM, Zhang W, Hearn S, Elemento O, Paknejad N, Manova-Todorova K, Welte K, Bromberg J, Peinado H, Lyden D (2014) Double-stranded DNA in exosomes: a novel biomarker in cancer detection. Cell Res 24:766–769
12. Peinado H, Aleckovic M, Lavotshkin S, Matei I, Costa-Silva B, Moreno-Bueno G, Hergueta-Redondo M, Williams C, Garcia-Santos G, Ghajar C, Nitadori-Hoshino A, Hoffman C, Badal K, Garcia BA, Callahan MK, Yuan J, Martins VR, Skog J, Kaplan RN, Brady MS, Wolchok JD, Chapman PB, Kang Y, Bromberg J, Lyden D (2012) Melanoma exosomes educate bone marrow progenitor cells toward a pro-metastatic phenotype through MET. Nat Med 18:883–891
13. Pando A, Reagan JL, Quesenberry P, Fast LD (2018) Extracellular vesicles in leukemia. Leuk Res 64:52–60
14. Szczepanski MJ, Szajnik M, Welsh A, Whiteside TL, Boyiadzis M (2011) Blast-derived microvesicles in sera from patients with acute myeloid leukemia suppress natural killer cell function via membrane-associated transforming growth factor-beta1. Haematologica 96:1302–1309
15. Caivano A, Laurenzana I, De Luca L, La Rocca F, Simeon V, Trino S, D'Auria F, Traficante A, Maietti M, Izzo T, D'Arena G, Mansueto G, Pietrantuono G, Laurenti L, Musto P, Del Vecchio L (2015) High serum levels of extracellular vesicles expressing malignancy-related markers are released in patients with various types of hematological neoplastic disorders. Tumour Biol 36: 9739–9752
16. Caivano A, La Rocca F, Simeon V, Girasole M, Dinarelli S, Laurenzana I, De Stradis A, De Luca L, Trino S, Traficante A, D'Arena G, Mansueto G, Villani O, Pietrantuono G, Laurenti L, Del Vecchio L, Musto P (2017) MicroRNA-155 in serum-derived extracellular vesicles as a potential biomarker for hematologic malignancies - a short report. Cell Oncol (Dordr) 40:97–103
17. Huan J, Hornick NI, Shurtleff MJ, Skinner AM, Goloviznina NA, Roberts CT Jr, Kurre P (2013) RNA trafficking by acute myelogenous leukemia exosomes. Cancer Res 73:918–929
18. Hong CS, Muller L, Whiteside TL, Boyiadzis M (2014) Plasma exosomes as markers of therapeutic response in patients with acute myeloid leukemia. Front Immunol 5:160

3.2 Evaluation of dsDNA from extracellular vesicles in pediatric AML diagnostics.

Annals of Hematology (2020) 99:459–475
https://doi.org/10.1007/s00277-019-03866-w

ORIGINAL ARTICLE

Evaluation of dsDNA from extracellular vesicles (EVs) in pediatric AML diagnostics

Evangelia Kontopoulou[1] · Sarah Strachan[1] · Katarina Reinhardt[1] · Fabienne Kunz[1] · Christiane Walter[1] · Bernd Walkenfort[2] · Holger Jastrow[3] · Mike Hasenberg[2] · Bernd Giebel[4] · Nils von Neuhoff[1] · Dirk Reinhardt[1] · Basant Kumar Thakur[1]

Received: 30 July 2019 / Accepted: 20 November 2019 / Published online: 13 January 2020

Abstract

Acute myeloid leukemia (AML) is a heterogeneous malignant disease characterized by a collection of genetic and epigenetic changes. As a consequence, AML can evolve towards more aggressive subtypes during treatment, which require additional therapies to prevent future relapse. As we have previously detected double-stranded DNA (dsDNA) in tumor-derived extracellular vesicles (EVs), in this current study we attempted to evaluate the potential diagnostic applications of AML EV-dsDNA derived from primary bone marrow and peripheral blood plasma samples. EVs from plasma of 29 pediatric AML patients (at initial diagnosis or during treatment) were isolated by ultracentrifugation, after which dsDNA was extracted from obtained EVs and analyzed for leukemia-specific mutations using next generation sequencing (NGS) and GeneScan-based fragment-length analysis. In 18 out of 20 patients, dsDNA harvested from EVs mirrored the (leukemia-specific) mutations found in the genomic DNA obtained from primary leukemia cells. In the nanoparticle tracking analysis (NTA), a decrease in EV numbers was observed in patients after treatment compared with initial diagnosis. Following treatment, in 75 samples out of the 79, these mutations were no longer detectable in EV-dsDNA. In light of our results, we propose the use of leukemia-derived EV-dsDNA as an additional measure for mutational status and, potentially, treatment response in pediatric AML.

Keywords Acute myeloid leukemia · EVs · dsDNA · Mutational detection · Pediatrics

Introduction

Acute myeloid leukemia (AML) is the second most common form of pediatric leukemia, with relapse rates of more than 30% in all patients. Clonal evolution of rare primary leukemic cells, which survived initial therapy or gained additional mutations, is considered as a potential cause of relapse in pediatric AML [1, 2]. With the recent advancements in the field of cancer genomics (e.g., whole genome deep sequencing at the single cell level), it has become clear that genomes acquire AML mutations in a stepwise manner, leading to the presence of genetically heterogeneous populations of leukemic cells in the hematopoietic compartment [2]. Due to this biological heterogeneity at the genomic DNA level, it is a great challenge to clinically target AML and to achieve a disease-free state in patients. In recent years, research has been intensively focused on understanding the process of clonal evolution in leukemia progression, both during therapy and relapse, as relapse remains the major cause of lethality in pediatric AML [3].

Classically, the role of extracellular signalling molecules, such as cytokines and growth factors, released by leukemic cells, has been discussed to modulate the microenvironment towards leukemogenesis [4, 5]. In the last decade, extracellular vesicles (EVs), especially exosomes and microvesicles, have been shown to mediate complex intercellular interactions

Electronic supplementary material The online version of this article (https://doi.org/10.1007/s00277-019-03866-w) contains supplementary material, which is available to authorized users.

✉ Basant Kumar Thakur
basant-kumar.thakur@uk-essen.de

[1] Department of Pediatric Hematology and Oncology, University Children's Hospital, University Hospital of Essen, Hufelandstrasse 55, 45147 Essen, Germany

[2] Imaging Centre Essen, Electron Microscopy Unit, University Hospital of Essen, Essen, Germany

[3] Institute of Anatomy, University Hospital of Essen, Essen, Germany

[4] Institute of Transfusion Medicine, University Hospital of Essen, Essen, Germany

at local and distant sites, in normal and pathophysiological conditions [6]. EV preparations contain many important biomolecules including nucleic acids (DNA, mRNA, and microRNA), proteins, and lipids [7–10], which can be transferred from EV releasing cells to their specific target cells [11]. Containing cell type–specific signatures, EVs and their cargo molecules have a huge potential to serve as novel biomarkers for a variety of different diseases [12]. Indeed, we and others previously demonstrated that EV preparations of various tumor patients contained dsDNA which mirrored the mutational information of the tumor cells from which they were produced [13–19].

The aim of the current study was to evaluate the potential diagnostic role of leukemia-derived EVs in pediatric AML. Accordingly, we harvested EVs from the plasma of AML patients, extracted their dsDNA, and analyzed it for AML-specific mutations using AML-specific next-generation sequencing (NGS) as well as GeneScan-based fragment-length analysis. Although it has been previously shown that in AML plasma EV number correlates with leukemic blood cell counts, and that miRNA from EVs has potential as a biomarker for minimal residual disease (MRD) and patient prognosis [20–22], the data that we have been able to generate in this study is the first to show the potential diagnostic applications of EV-dsDNA in primary AML pediatric patient samples.

Materials and methods

Twenty-nine patients with AML (Supplementary Table S1) were included in our study. Genetic information and the levels of hemoglobin, leukocytes, and myeloblasts of each patient are provided (Table 1 and Supplementary Table S1). Each patient was consented following institutional review board approval AML-BFM 2004 (3VCreutzig1). The age of the patients ranged from less than 1 up to 18 years. As a reference point, the plasma from 5 healthy donors between 25 and 40 years old were also collected. Plasma (1–2 mL) from bone marrow (BM) or peripheral blood (PB) was collected from each patient prior to the start of chemotherapy (twenty-nine patients) as well as after different stages of chemotherapy (twenty patients) (Table 1), and 7 mL peripheral blood from each healthy donor were collected at one time point. EVs were isolated using a differential ultracentrifugation protocol (Supplementary Figure S1). The number of EVs and their diameter were quantified by nanoparticle tracking analysis (NTA) using ZetaView (Particle Metrix GmbH). The dsDNA was isolated to allow genomic and EV-DNA sequencing for tumor profiling using MiSeqDx (Illumina Inc.) with the TruSight Myeloid (TSM) panel (Illumina, FC-130-1010) using the MiSeq V2 Reagent kit (2 × 150 cycles, paired end run) and a total of 141 kb per sample, as well as with GeneScan-based fragment-length analysis (Supplementary Figure S1). All statistical analyses were performed using Prism 7 (GraphPad, San Diego). Data were analyzed using unpaired and paired Student's *t* test. The majority of results are expressed as means including the standard deviation with $P < 0.05$ being considered statistically significant.

Ultracentrifugation of patient samples and healthy donor samples

Healthy donor blood (7 mL) was collected in red-top EDTA (ethylenediamine tetraacetic acid) tubes (#01.1605.001, SARSTEDT AG & Co. KG). Plasma samples from patients with childhood AML were obtained from the Biobank. The EVs from the healthy donors and the patient samples were isolated using 3 steps of differential centrifugation followed by ultracentrifugation according to the protocol from Kunz et al 2019 [23].

From each plasma sample, 200 μL were transferred into new microcentrifuge tubes and stored at − 80 °C as a control before EV depletion (unfractionated plasma). The supernatants after the first spin of 100,000×*g* were collected in fresh microcentrifuge tubes and stored at − 80 °C for future analysis of DNA in the plasma after EV depletion (fractionated plasma). The final EV pellet was resuspended in 200 μL of PBS. From the obtained EV fraction, 20 μL were used for the Transmission Electron Miroscopy (TEM), BCA assay, and ZetaView analysis. The rest of the samples were stored at − 80 °C for later Western blot analysis as well as DNA isolation and sequencing (Supplementary Figure S1).

ZetaView analysis-nanoparticle tracking analysis

EV size and concentration were analyzed by nanoparticle tracking analysis using the ZetaView device of Particle Metrix. Firstly, 100 nm "Standard beads" (Particle Metrix GmbH) were used to calibrate the machine. The following settings were used for all measurements: 11 positions, 5 cycles, medium quality, minimal brightness of 20, minimal size of 5 nm, maximal size of 200 nm, tracelength of 15 s, sensitivity of 75%, shutter speed of 75 ms, and a frame rate of 30. Sample dilutions were adjusted using DPBS (#14200075, ThermoFischer Scientific) to a final volume of 1 mL. For analysis, size and concentration of particles were determined using Software provided by Zetaview (version 2.3) (Particle Metrix GmbH).

Transmission electron microscopy

TEM was performed at the Electron Microscopy Unit (EMU) of the Imaging Center Essen (IMCES) to visualize the EVs. First of all, 3 μL of isolated EV fractions were added on to a Formvar-coated 200 mesh copper grid (#SF162, PLANO GmbH). The grid had been previously prepared by making

Table 1 AML patients' samples overview and mutational analysis

Patient number	Age at diagnosis (years)	FAB	% blasts	Leukocytes (103)	Hb (g/dl)	Date	Material	Remark treatment block	Mutations gDNA	Mutations EV-DNA
1	16	M1	BM: 90% PB: 90%	67.5	10.2	09.05.2016	PB	Initial	WT1 NPM1 FLT3-TKD GATA2 ETV6(SNP) ZRSR2(SNP)	WT1 NPM1 FLT3-TKD GATA2 ETV6(SNP) ZRSR2(SNP)
1a			BM: 79% PB: n.a	0.1	6.9		BM	After ADxE	n.a n.a n.a n.a n.a n.a	* * * * * *
1b			BM: 81% PB: n.a	0.1	7.8		BM	After ADxE	n.a n.a n.a n.a n.a n.a	n.d * n.d * n.d * n.d * n.d * n.d *
1c			BM: 0% PB: 0%	2.2	8.2		BM	After HAM	n.a n.a n.a n.a n.a n.a	n.d n.d n.d n.d ETV6(SNP) ZRSR2(SNP)
1d			BM: 0% PB: 0%	1.9	9.5		BM	After AI	n.a n.a n.a n.a n.a n.a	n.d n.d n.d n.d ETV6(SNP) ZRSR2(SNP)
1e			BM: 0% PB: 0%	3.7	10.2		BM	After hAM	n.a n.a n.a n.a n.a n.a	n.a n.a n.a n.a n.a n.a
2	5	M2	BM: 30% PB: 23%	7.3	7.9	20.12.2016	BM	Initial	t(8;21), FLT3-ITD, RAD21, KIT, EZH2	n.d n.d n.d n.d
2a			BM: 0% PB: 0%	0.6	7.5		BM	After ADxE	t(8;21), FLT3-ITD, RAD21, KIT, EZH2	n.d * n.d * n.d * n.d *
2b			BM: 0% PB: 0%	2.8	9.5		BM	After AI	n.d n.d n.d n.d n.d	n.a n.a n.a n.a n.a
2c			BM: 0% PB: 0%	2.3	8.1		BM	After hAM	n.d n.d n.d n.d	* * * *
3	18	M3	BM: 71% PB: 3%	0.9	7.5	28.06.2016	PB	Initial	t(15;17) GATA2(SNP) NOTCH1(SNP)	t(15;17) GATA2(SNP) NOTCH1(SNP)
3a			BM: 0% PB: 0%	48	8.6		BM	After block 2	t(15;17) GATA2(SNP) NOTCH1(SNP)	n.d GATA2(SNP) NOTCH1(SNP)
3b			BM: 0% PB: 0%	5.8	12.4		BM	After ATRA	n.d n.d n.d	n.d GATA2(SNP) NOTCH1(SNP)
3c			BM: 0%	3.6	11.8		BM	After block 4	n.d	n.d

Table 1 (continued)

Patient number	Age at diagnosis (years)	FAB	% blasts	Leukocytes (103)	Hb (g/dl)	Date	Material	Remark treatment block	Mutations gDNA	Mutations EV-DNA
			PB: 0%						n.d	GATA2(SNP)
									n.d	NOTCH1(SNP)
3d			BM: 0%	No data	No data		BM	After block 5 ATO	n.d	n.d
			PB: 0%						n.d	GATA2(SNP)
									n.d	NOTCH1(SNP)
4	1	M4	BM: 83%	11	8.6	29.11.2016	BM	Initial	t(1;11)	t(1;11)
			PB: 25%						NRAS	NRAS
									KIT (SNP)	KIT (SNP)
									PHF6 (SNP)	PHF6 (SNP)
4a			BM: 5%	0.2	6.1		BM	After d26	t(1;11)	n.d
			PB: n.a						NRAS	n.d
									KIT (SNP)	KIT (SNP)
									PHF6 (SNP)	PHF6 (SNP)
4b			BM: 0%	1.7	9.1		BM	After AI	n.d	n.d
			PB: 0%						n.d	n.d
									n.d	KIT (SNP)
									n.d	PHF6 (SNP)
14	9	M1	BM: 78%	51.75	7.8	26.09.2017	BM	Initial	FLT3-ITD	FLT3-ITD
			PB: 88%							
14a			BM: 0%	0.1	7.1	23.10.2017	BM	After 1 induction	n.a	n.d
			PB: n.a							
14b			BM: 0%	1.89	7.9	30.10.2017	BM	After CDxA	FLT3-WT	n.d
			PB: 0%							
14c			BM: 0%	n.a	n.a	21.12.2017	BM	After HAM	FLT3-WT	n.d
			PB: n.a							
15	4	M2	BM: 45%	9.86	7.3	13.01.2017	BM	Initial left	FLT3-ITD	n.d
			PB: 0%							
15a			BM: 34%	9.86	7.3	13.01.2017	BM	Initial right	FLT3-ITD	n.d
			PB: n.a							
15b			BM: 0%	3.15	9.6	21.03.2017	BM	After AI	FLT3-WT	n.d
			PB: 0%							
15c			BM: 0%	3.3	11.5	19.04.2017	BM	After HAM	FLT3-WT	n.d
			PB: n.a							
15d			BM: 0%	3.5	9.5	18.05.2017	BM	After HAM	FLT3-WT	n.d
			PB: 0%							
15e			BM: 0%	5.36	11.0	06.07.2017	BM	After HAE	FLT3-WT	n.d
			PB: n.a							
16	4	M1	BM: 93%	16.1	9.5	28.08.2017	BM	Initial	FLT3-ITD	FLT3-ITD
			PB: 50%						NPM1	NPM1
16a			BM: 2%	0.6	10.1	21.09.2017	BM	After ADxE	FLT3-ITD	n.d
			PB: n.a						NPM1	n.d
16b			BM: 0%	3.0	9.0	04.10.2017	BM	After ADxE 1st total remission	FLT3-WT	n.d
			PB: 0%						NPM1-WT	n.d
16c			BM: 0%	3.1	9.6	30.10.2017	BM	After HAM Remission	FLT3-WT	n.d
			PB: 0%						NPM1-WT	n.d
16d			BM: 0%	2.7	9.1	02.01.2018	BM	After AI Remission	FLT3-WT	n.d
			PB: 0%						NPM1-WT	n.d
17	2	M1	BM: 94%	9.7	8.4	22.08.2016	BM	Initial	NPM1	NPM1
			PB: n.a							
17a			PB: 56%	n.a	n.a	22.08.2016	PB	Initial	NPM1	NPM1
			PB: n.a							
17b			BM: 19%	0.2	10.0	13.09.2016	BM	After ADxE	NPM1	n.d
			PB: n.a							
17c			BM: 0%	2.3	9.7	21.09.2016	BM	After CDxA	NPM1-WT	n.d
			PB: n.a							
17d			BM: 0%	4.9	13.4	01.03.2017	BM	After HAE	NPM1-WT	n.d
			PB: n.a							
17e			BM: 0%	3.2	12.2	27.11.2017	BM	Suspected relapse	NPM1-WT	n.d
			PB: n.a							
18	5	M2	BM: 33%	28.7	5.7	12.12.2017	BM	Initial	NPM1	NPM1
			PB: 8%							
18a			BM: 16%	0.6	11.6	02.01.2018	BM	After AIE	NPM1	n.d
			PB: 0%							

Table 1 (continued)

Patient number	Age at diagnosis (years)	FAB	% blasts	Leukocytes (103)	Hb (g/dl)	Date	Material	Remark treatment block	Mutations gDNA	Mutations EV-DNA
18b			BM: 0% PB: 0%	2.4	13.2	25.01.2018	BM	After HAM	NPM1-WT	n.d
19	15	M5	BM: 79% PB: 11%	6.55	7.0	26.01.2017	BM	Initial	FLT3-ITD	FLT3-ITD
19a			n.a	0.01	7.4	30.03.2017	BM	After HAM	FLT3-ITD	n.d
19b			BM: 0% PB: n.a	1.13	8.5	02.05.2017	BM	After HAM	FLT3-WT	n.d
19c			BM: 0% PB: 0%	1.05	9.0	05.07.2017	BM	After HAM	FLT3-WT	n.d
19d			BM: 0% PB: n.a	0.73	8.0	29.08.2017	BM	After HAE	FLT3-WT	n.d
19e			BM: 0% PB: 0%	0.29	8.0	05.10.2017	BM	After HAE	FLT3-WT	n.d
19f			BM: 0% PB: n.a	3.33	12.2	02.11.2017	BM	After DT	FLT3-WT	n.d
19g			BM: 0% PB: 0%	0.45	10.0	21.12.2017	BM	After DT	FLT3-WT	n.d
20	7	M2	BM: 81% PB: 47%	37.24	61.9	11.09.2017	BM	Initial	NPM1	NPM1
20a			BM: 0% PB: n.a	0.37	8.6	21.09.2017	BM	After ADxE	NPM1	NPM1
20b			BM: 0% PB: n.a	0.35	10.2	05.10.2017	BM	After ADxE	NPM1	n.d
20c			BM: n.a PB: n.a	3.82	9.8	16.10.2017	BM	After ADxE 1st remission	NPM1	n.d
20d			BM: 0% PB: n.a	2.54	11.9	14.11.2017	BM	After HAM	NPM1	n.d
20e			BM: 0% PB: 0%	2.86	11.3	12.12.2017	BM	n.a	NPM1	n.d
20f			BM: 0% PB: 0%	2.81	8.8	11.01.2018	BM	Still in remission After HA(E)	NPM1	n.d
20g			n.a	n.a	n.a	13.02.2018	BM	n.a	NPM1-WT	n.d
21	18	M2	BM: 58% PB: 62%	21.0	8.0	04.08.2017	BM	Initial	FLT3-ITD	FLT3-ITD
21a			BM: 14% PB: n.a	1.0	8.3	28.08.2017	BM	After Dag-21	n.a	FLT3-ITD
21b			BM: 0% PB: 0%	1.12	7.5	04.10.2017	BM	After HAM	n.a	n.d
21c			BM: 0% PB: n.a	1.99	9.3	09.10.2017	BM	After AI	n.a	n.d
21d			BM: 0% PB: n.a	1.98	11.5	23.11.2017	BM	After AI	FLT3-WT	n.d
22	14	M6	BM: 20% PB: 5%	8.4	6.1	28.03.2017	BM	Initial	NPM1	NPM1
22a			BM: 14% PB: n.a	6.81	6.2	03.04.2017	BM	Initial	NPM1	n.a
23	17	M5	BM: 91% PB: 35%	32.86	9.7	25.07.2017	BM	Initial	FLT3-ITD, NPM1	FLT3-ITD NPM1
23a			BM: 0% PB: n.a	0.69	9.2	16.08.2017	BM	After ADxE	FLT3-WT, NPM1	n.d n.d
23b			BM: 0% PB: n.a	2.05	7.3	28.08.2017	BM	After ADxE	FLT3-WT, NPM1	n.d n.d
23c			BM: 0% PB: n.a	2.37	8.7	31.08.2017	BM	After ADxE	FLT3-WT, NPM1	n.d n.d
23d			BM: 0% PB: n.a	3.44	9.5	13.11.2017	BM	After AI	FLT3-WT, NPM1-WT	n.d n.d
24	14	M4	BM: 66% PB: 40%	9.1	6.0	08.09.2017	BM	Initial	FLT3-ITD	FLT3-ITD
24a			BM: 0% PB: n.a	0.5	9.0	28.09.2017	BM	After CDxA	FLT3-WT	n.d
24b			BM: 0% PB: 0%	1.9	9.0	11.10.2017	BM	After CDxA	FLT3-WT	n.d
24c			BM: 0%	0.7	9.0	11.01.2018	BM		FLT3-WT	n.d

Table 1 (continued)

Patient number	Age at diagnosis (years)	FAB	% blasts	Leukocytes (103)	Hb (g/dl)	Date	Material	Remark treatment block	Mutations gDNA	Mutations EV-DNA
			PB: 0%					Day 28 after BM transplantation		
24d			BM: 0% PB: 0%	2.8	7.6	24.01.2018	BM	Day 40 after BM transplantation	FLT3-WT	n.d
25	14	M4	BM: 56% PB: 31%	23.18	5.1	15.09.2017	BM	Initial	FLT3-ITD	FLT3-ITD
25a			BM: 0% PB: 0%	1.25	9.6	23.10.2017	BM	After ADxE	FLT3-WT	n.d
25b			BM: 0% PB: 0%	1.57	8.3	n.a	BM	Before AI	FLT3-WT	n.d
26	16	M4	BM: 36% PB: 14%	8.0	13.4	04.08.2017	BM	Initial	FLT3-ITD	FLT3-ITD
26a			BM: 0% PB: 0%	0.8	12.0	04.09.2017	BM	After DNX-FLA	FLT3-WT	n.d
26b			BM: 0% PB: n.a	3.1	15.3	11.09.2017	BM	After DNX-FLA	FLT3-WT	n.d
26c			BM: 0% PB: 0%	1.19	7.8	06.02.2018	BM	Month 4 after BM transplantation	FLT3-WT	n.d
27	8	M2	BM: 45% PB: 19%	3.47	7.8	01.02.2018	BM	Initial	NPM1	NPM1
27a			BM: 0% PB: n.a	0.61	10.0	01.03.2018	BM	After AIE	NPM1-WT	n.d
27b			BM: 0% PB: n.a	1.33	11.2	09.04.2018	BM	After HAM	NPM1-WT	n.d
28	7	M1	BM: 87% PB: 91%	37.8	7.7	02.03.2018	BM	Initial relapse	NPM1	NPM1
28a			BM: 96% PB: n.a	0.47	8.2	03.04.2018	BM	Day 28 relapse	NPM1	n.d
28b			BM: 0% PB: n.a	0.45	10.0	26.04.2018	BM	After Clofarabine	NPM1	n.d
29	15	M2	BM: 84% PB: 80%	24.53	15.8	22.11.2017	BM	Initial	NPM1	NPM1
29a			BM: 0% PB: n.a	0.67	10.0	13.12.2017	BM	Day 21	NPM1	n.d
29b			BM: 0% PB: n.a	1.93	9.3	19.02.2018	BM	After AI	NPM1-WT	NPM1*

Information of all the collected samples. Next-generation sequencing analysis of known mutations and GeneScan-based fragment-length analysis of FLT3-ITD and NPM1 (insertion) mutations were performed to investigate the diagnostic potential of DNA that was extracted from EVs. The results were compared with the actual mutational status of the patients that was obtained from the already existing primary leukemia database in the AML-BFM lab. Four patient samples (P1–P4) from before and after treatment were used for NGS analysis. For the sequencing, 50 ng or a maximum volume of 15 μL was used from each sample depending on their concentration. AML-specific mutations were not present in post-treatment samples. SNPs were present in all analyzed samples

Sixteen patient samples (P14–P29) from before and after treatment were used for GeneScan-based fragment-length analysis. 50 ng/μL or a maximum volume of 10.5 μL from each sample was used depending on their concentration. AML-specific mutations were not present in post-treatment samples. Any "positive" or "negative" entries are mentioned by the name of the mutations or a note that the mutations were not detectable (n.d) or not applicable (n.a). *= Low quality sequencing data

its surface hydrophilic using glow discharging for 1.5 min (easiGlow™, PELCO). Samples were then negatively stained with 10 μL of 1.5% v/v Phosphotungstic acid (PTA) for 2 min, after which excess liquid was removed. The grids were allowed to dry for at least 2 min and then observed with a JEOL JEM-1400 Plus TEM (JEOL) at 120 kV. Additional positive staining was performed for extra validation of our results. For this, 7.5 μL of isolated EV fractions were mixed and positively stained with 1.5 μL of 1% Methyl-cellulose and 1 μL of 1% Uranyl-acetate and incubated at room temperature for 30 min. From this mixture, 1.5 μL were added on to a Formvar-coated 200 mesh copper grid (#SF162, PLANO GmbH) which had been previously prepared by making its surface hydrophilic using glow discharging for 1.5 min (easiGlow™, PELCO). Samples were dried on the grid for 2 min and then observed with a JEOL JEM-1400 Plus TEM (JEOL) at 120 kV. 4K images were acquired with TemCam-F416 and EM-Menu 4 software (TVIPS GmbH).

Protein concentration analysis

A bicinchoninic acid assay (BCA) was performed using a BCA protein assay kit (#23225, ThermoFischer Scientific) according to the manufacturer's instructions. Protein concentrations were determined using the modulus microplate reader (Turner Biosystems) at a wavelength of 562 nm.

Western blots

Equal volumes of EV fractions from leukemia cell lines (MV4-11 and OCI-AML3 served as controls), healthy donors, and patient samples were treated 1:1 with RIPA buffer containing protease (cOmplete, #11697498001, Hoffman-La Roche) and phosphatase (PhosphoSTOP, #04906837001, Hoffman-La Roche) inhibitors. Next, 25 μl of the EV fractions were added to a master mix of β-mercaptoethanol (M-7522, Sigma-Aldrich) and 6× SDS Protein Loading Buffer pH 6.8 (#LB0100, Morganville Scientific), heated at 95 °C for 10 min, then loaded on to NuPAGE 4–12% Gels (#NPO321Box, Invitrogen, ThermoFischer Scientific) with the PageRuler Prestained protein ladder (#26616, ThermoFischer Scientific) for separation. THP-1 Cell Lysate (#sc-2238, Santa Cruz) was used as a control to verify the leukemia origin of the patient plasma-derived EVs and 20 μl were loaded directly to the gel after heaingt at 95 °C for 10 min. Afterwards, they were transferred on to a nitrocellulose blotting membrane (#10600001, GE Healthcare). After transfer, membranes were washed with TBS-T and blocked in 5% milk blocking solution with 0.05% Tween-20 for 30 min. The membranes were then incubated overnight at 4 °C with primary antibodies in 5% milk blocking solution (1:1000): Anti-CD63 (#EXOAB-KIT-1, System Biosciences), Anti-HSP70 (#EXOAB-KIT-1, System Biosciences), Anti-TSG101 (#HPA006161, Sigma-Aldrich), Anti-Syntenin (#ab133267, Abcam), Anti-CD33 (ab134115, Abcam), and Anti-CD13 (ab108310, Abcam). Next day, membranes were washed with TBS-T and incubated at RT for 90 min with the relevant secondary antibody (1:10,000 for the Anti-Rabbit IgG, HRP-linked Antibody, #7074S, Cell Signalling) or (1:20,000 for the Goat Anti-rabbit HRP, #EXOAB-KIT-1, System Biosciences). After washing, blots were developed with ECL Prime Western Blotting Detection reagents (#2232, GE Healthcare) and detected with a Fusion FX Machine (Vilber Lourmat Deutschland GmbH).

QIAamp DNA Micro Kit

DNA was extracted from plasma samples, EVs, and EV supernatants using the QIAamp DNA Micro Kit (#56304, Qiagen) according to the manufacturer's instructions. Briefly, 100 μL from each sample was pipetted into a 1.5-mL microcentrifuge tube with 4 μL of RNase (#56304, Qiagen) and incubated at RT for 15 min. Next, 100 μL of Buffer AL (#56304, Qiagen) was added, followed by vortexing for 15 s. Then, 10 μL proteinase K (#56304, Qiagen) was added and the samples were incubated at 56 °C for 10 min. Afterwards, 100 μL of ethanol 100% (#603-002-00-5, Honeywell Riedel-de Haën AG) were added followed by vortexing for 15 s. The samples were transferred into a QIAamp MinElute (#56304, Qiagen) column after 3 min incubation at RT. Centrifugation steps of 6000×*g* for 1 min were performed in between the washing steps with 500 μl of each washing buffer: AW1 (#56304, Qiagen) and AW2 (#56304, Qiagen). The columns were transferred into clean 1.5-mL microcentrifuge tubes and 50 μL of distilled water were applied to the center of each membrane, followed by centrifugation at full speed (20,000×*g*) for 1 min, to elute the DNA. From each eluted sample, 1 μL was used to perform Qubit or dsDNA quantifluor for the measurement of concentration. The samples were stored at − 80 °C.

DNA quantification

The dsDNA from 4 patients, unfractionated plasma, and EVs were measured using Qubit 3.0 Fluorometer (#Q33226, ThermoFischer Scientific) according to the manufacturer's instructions. Briefly, Qubit® working solution was prepared by diluting the Qubit® reagent (#Q33227, ThermoFischer Scientific) 1:200 in Qubit® buffer (#Q33227, ThermoFischer Scientific). Two Assay tubes (#Q32856, ThermoFischer Scientific) for the standards (190 μL working solution + 10 μL standards) and one for each sample (199 μL working solution + 1 μL sample) were prepared. Tubes were inserted into a Qubit® fluorometer for analysis. The dsDNA from all fractions of the remaining 25 patient samples were quantified using a dsDNA quantifluor kit (#ab27156, Promega) according to manufacturer's instructions. Briefly, 1× TE buffer, dsDNA dye working solution and standards were prepared. Next, 200 μL of dsDNA dye working solution was applied to each well (standard, blank and sample). Then, 10 μL of the standards, 10 μL 1× TE buffer for the blank or 1 μL of each sample was added. The plate was mixed thoroughly and incubated for 5 min at RT. Plate was analyzed using fluorescence (504 nm_{Ex}/531 nm_{Em}) by the modulus microplate reader (Turner Biosystems).

DNA bioanalysis

The EV-DNA fragment sizes from patient samples and healthy donor samples were analyzed using an Agilent High Sensitivity D1000 ScreenTape Assay. Briefly, a ladder was prepared by adding 2 μL High Sensitivity D1000 sample buffer and 2 μL High Sensitivity D1000 ladder (#0006371807, Agilent Technologies) in a tube strip (#0200794-260, Agilent Technologies). Samples were then

prepared by adding 2 μL High Sensitivity D1000 sample buffer and 2 μL of each sample in a tube strip. The tube strips were then covered by caps (#401425, Agilent Technologies) and mixed by vortexing for 1 min and then briefly spun down. The tube strips were then loaded in to the Agilent 4200 TapeStation instrument (4200 TapeStation, Agilent Technologies) and the caps removed. Results were then generated using the Agilent Tapestation Analysis Software.

Sequencing of patient samples

The DNA samples that were measured using the Qubit 3.0 Fluorometer (ThermoFischer Scientific) were sequenced using Next Generation Sequencing-Illumina MiSeqDx (Illumina Inc.). For targeted sequencing with the TruSight Myeloid (TSM) panel (FC-130-1010, Illumina Inc.) (Table 2), 50 ng of DNA derived from bulk bone marrow or peripheral blood cells at diagnosis were used by the AML-BFM central core facility. The plasma and EV-DNA sequencing was performed using either 50 ng of DNA or, for the samples with low concentration, a maximum volume of up to 15 μL. The libraries were prepared according to the manufacturer's protocol and sequenced with Illumina MiSeqDx using the MiSeq V2 Reagent kit (2 × 150 cycles, paired end run) (MS-102-2002, Illumina Inc.), with a total of 141 kb per sample.

GeneScan-based fragment-length analysis

The DNA from the last sixteen patients was measured using a dsDNA quantifluor kit (#ab27156, Promega) and underwent mutational detection with GeneScan-based fragment-length analysis. A master mix of reagents was prepared: Hot Start Taq 2x MM 12.5 μL, DEPC H_2O 8.5 μL, Primer F (10 pmol/μL) 1 μL, Primer R (10 pmol/μL) 1 μL. A DNA concentration of 50 ng/μL or a maximum volume of 10.5 μL of sample was used. Water can be avoided in case of 10.5 μL of DNA. For amplification, samples were heated at 95 °C for 2 min, followed by 40 cycles of 95 °C for 15 s, 59 °C for 15 s and 72 °C for 15 s. GeneScan-based fragment-length analysis was performed for the FLT3-Internal Tandem Repeat (FLT3) and Nucleophosphomin (NPM1) mutations by using the following primers:

FLT3-ITD:

Primer fw: 5′-GTAAAACGACGGCCAGGCAA TTTAGGTATGAAAGCCAGC-3′
Primer rev: 5′-FAM-CTT TCA GCA TTT TGA CGG CAA CC-3′

NPM1:

Primer fw: 5′-GTAAAACGACGGCCAGGATG TCTATGAAGTGTTGTGGTTCC-3′
Primer rev: 5′-VIC-ATC AAA CAC GGT AGG GAA AGT TC-3′

PCR products were diluted (1:70) in H_2O. One microliter of diluted PCR products was mixed with 10 μL HiDi Formamid (Applied Biosystems) and 0.3 μL GeneScan 600 LIZ Size Standard v 2.0 (ThermoFischer Scientific). PCR products were denaturated for 5 min at 95 °C and the GeneScan-based fragment-length analysis was performed using the 3500 genetic analyzer (Applied Biosystems).

Results

Characterization of EV preparations

To characterize the EV content of plasma from pediatric AML samples, EVs were harvested by differential centrifugation/ultracentrifugation steps. Obtained EV fractions were characterized by nanoparticle tracking analysis (NTA) for the number and average diameter of obtained particles, while BCA assay was also performed to support the NTA quantification with additional protein quantification data, with a strong correlation between the two parameters being observed (Supplementary Figure 2; Supplementary Table S2). Average particle sizes obtained from AML patient plasma samples were in the range of 30–150 nm, the expected size of EVs (Figure 1a, b). To confirm the presence of EVs, transmission electron microscopy was performed. Bona fide EVs were indeed observed in all preparations studied (Fig. 1c–f). The presence of EVs in our preparations was further proven by Western blotting using EV-specific antibodies (Fig. 2a). EVs from leukemia cell lines which served as positive controls showed clear bands with the EV-specific antibodies. Furthermore, the origin of the EVs was confirmed by additional Western blots using myeloid-specific antibodies, which were present in the positive control as well as in the leukemia patient samples (Fig. 2b). For reference, EVs from healthy donors were also probed with the same myeloid-specific antibodies, which gave negative results (Fig. 2b). Healthy donor samples were also probed with EV-specific antibodies, but it was not possible to detect all tested antibodies. However, this could be explained by the lower number of EVs present in healthy donor samples in comparison to patient samples as the number of particles measured by NTA appeared to be statistically significantly higher in patient plasma samples than in healthy donor samples ["p" = 0.0057] (Supplementary Figure S3), and the same volume of EV fractions and not equal protein amount was loaded for Western blot analysis. As the healthy donor samples were from adults, this significant difference in EV

Table 2 Target regions of the TruSight Myeloid panel (Illumina)

Gene	Target region (exon)	Gene	Target region (exon)	Gene	Target region (exon)	Gene	Target region (exon)
ABL	4–6	DNMT3A	Full	KDM6A	Full	RAD21	Full
ASXL1	12	ETV6/Tel	Full	KIT	2, 8–11, 13+17	RUNX1	Full
ATRX	8–10 and 17–31	EZH2	Full	KRAS	2+3	SETBP1	4 (partial)
BCOR	Full	FBXW7	9+10+11	MLL	5–8	SF3B1	13–16
BCORL	Full	FLT3	14+15+20	MPL	10	SMC1A	2, 11, 16+17
BRAF	15	GATA1	2	MYD88	3–5	SMC3	10, 13, 19, 23, 25+28
CALR	9	GATA2	2–6	NOTCH1	26–29+34	SRSF2	1
CBL	8+9	GNAS	8+9	NPM1	12	STAG2	Full
CBLB	9, 10	HRAS	2+3	NRAS	2+3	TET2	3–11
CBLC	9, 10	IDH1	4	PDGFRA	12, 14, 18	TP53	2–11
CDKN2A	Full	IDH2	4	PHF6	Full	U2AF1	2+6
CEBPA	Full	IKZF1	Full	PTEN	5+7	WT1	7+9
CSF3R	14–17	JAK2	5+7	PTPN11	3+13	ZRSR2	Full
CUX1	Full	JAK3	3+13				

number cannot be fully concluded to be disease-related. Additionally, as normal myelopoiesis may be a rich source of EVs depending on regenerative activity and/or phases of cell destruction, our finding that steady-state PB of adults does not contain detectable amounts of myeloid EVs in Western blot experiments could be a matter of sensitivity and does not exclude that they could be detectable in other/better selected controls.

Analysis of EV numbers in pediatric AML samples at different stages of treatment

Next, we investigated whether EVs present in the plasma samples reflect the status of the leukemia blast burden in pediatric AML patients undergoing therapy. As proof of principle, we selected 20 of 29 patients in the study and isolated EVs from the selected patients' plasma samples at diagnosis and during different treatment blocks (Fig. 3). When comparing the particle numbers before and after treatment (all patients combined at each therapy block), lower particle numbers (although non-significant) were observed after treatment than before treatment ["p" = 0.084] (Fig. 3a). The number of leukemic blast cell burden was also declined during therapy; however, there was no correlation between the decrease of the amount of EVs and blasts (Table 1) (Supplementary Figure 4, and Supplementary Table S2). Analysis of EV numbers in individual patients before treatment and during different treatment blocks revealed a fluctuation of EV numbers in the plasma of patients, with a trend of an initial sharp decline and gradual increase during the time course of treatment (Fig. 3b–e).

EV samples from pediatric AML patients contain dsDNA reflecting AML-specific mutations

To establish the diagnostic relevance of EV-dsDNA isolated from pediatric AML patients, we isolated total DNA from EV fractions of our AML patients and, for comparison, from the unfractionated and fractionated plasma. Prior digestion of the DNA bound to the outside of EVs was not a pre-requirement in this study, as removing this DNA would have no diagnostic advantage for detecting mutations in EV-associated dsDNA. The DNA concentration was measured using Qubit (Fig. 4a) to quantify the amount for downstream NGS analysis. Additionally, dsDNA Quantifluor (Fig. 4b) was used to establish the double-stranded nature of EV-DNA, as demonstrated by Thakur et al. 2014 [13]. After isolation of EVs, we observed a lower concentration of dsDNA in EV-depleted (fractionated) plasma in comparison to unfractionated and EV fractions in the majority of patients in this study (Fig. 4a, b), validating the recent paper suggesting that majority of previously considered human blood plasma cell-free DNA is localized in EVs [24]. Additionally, in around 50% of the samples, the EV fractions contained more dsDNA than the initial unfractionated plasma (Fig. 4a, b). This could reflect that the DNA inside of the EVs is more protected than the cell-free DNA, which is vulnerable to degradation by nucleases in the plasma. In the next step, the dsDNA extracted from the initial samples, unfractionated plasma and EVs from patients 1, 2, 3, and 4, was sequenced using Illumina MiSeqDx (Supplementary Table S3). In three patients, identical mutations were detected in the EV-dsDNA and in the genomic DNA from the primary sample (gDNA) (Table 3). In one patient, mutations were only detectable

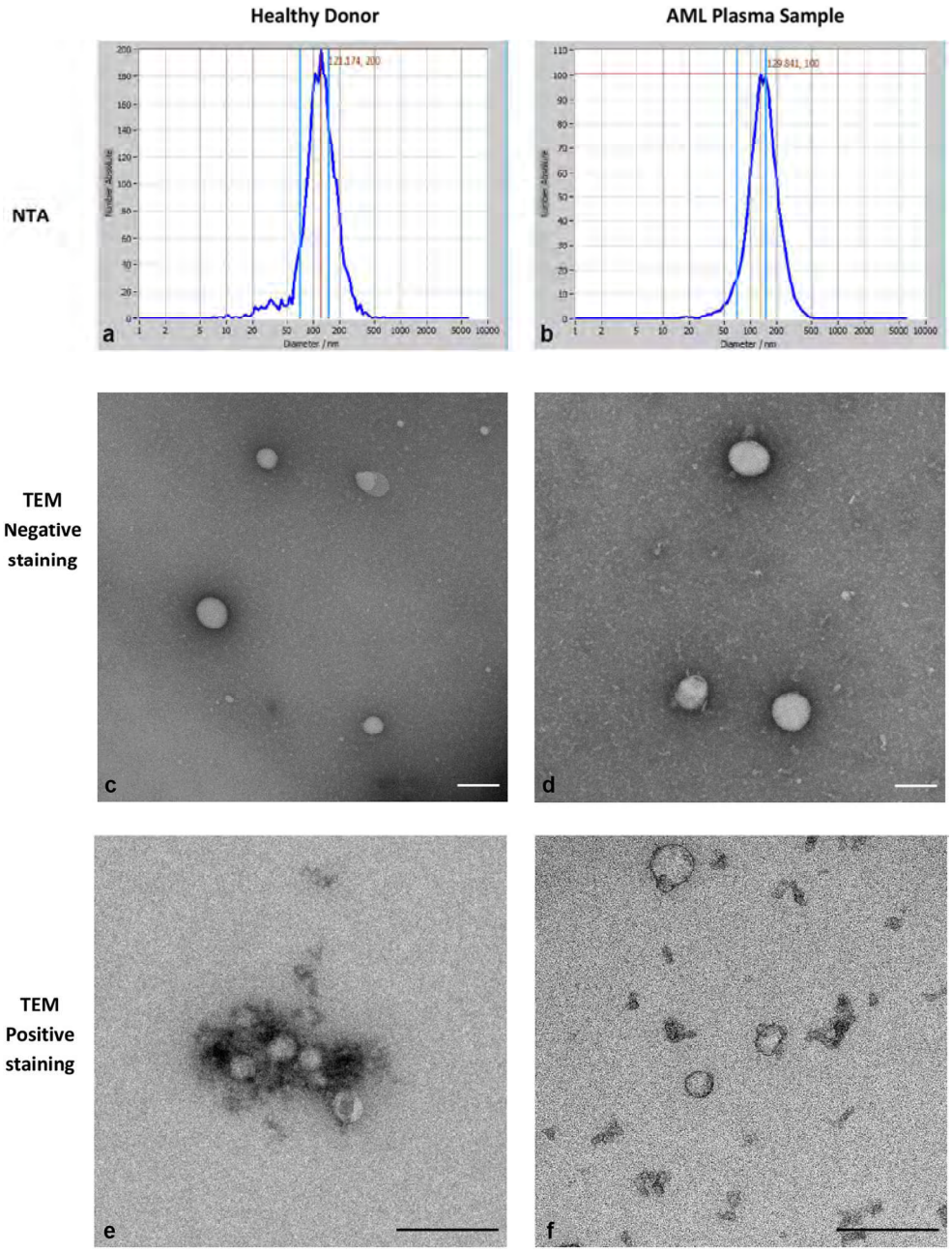

Fig. 1 Detection and characterization of EVs in healthy donor samples and patient samples. **a**, **b**) Exemplary data of Diameter size and number of particles per mL of plasma from healthy donor (HD) and AML patient samples (P), as measured by NTA. The size distribution is in the range of extracellular vesicles (30–150 nm). **c**, **d**) Exemplary data of TEM of negatively stained EVs from plasma of healthy donor samples and AML patient samples. Scale bar 200 nm. **e**, **f**) Exemplary data of TEM of positively stained EVs from plasma of healthy donor samples and AML patient samples. Scale bar 200 nm

in the gDNA and not in unfractionated plasma or EV-dsDNA (Table 3).

EV-derived dsDNA reflects therapy status based on mutational signature in pediatric AML

To gain insight into whether EV-dsDNA can be used to monitor the treatment response in pediatric AML patients, EV-dsDNA was isolated from patients before and after treatment. We observed that almost all AML patients in our study had higher dsDNA levels in EVs before therapy, compared with the EVs harvested from the same patients after therapy (Fig. 4c, d). The mutational background of the patients appeared to play a role in the EV-dsDNA concentration, as the samples from patients carrying only the FLT3-ITD mutation revealed a higher amount of dsDNA after treatment, while samples from patients that had an NPM1 mutation only or combined FLT3-ITD and NPM1 mutations showed decreased dsDNA concentration after treatment (Fig. 4e). The same trend was also observed with the EV number and RNA concentration [23]. In addition, to further characterize the EV-DNA, the DNA before and after treatment was analyzed using a bioanalyzer. This analysis revealed that in AML patients, four distinct DNA fragment sizes could be detected in EVs before treatment (Fig. 4f), but not after treatment

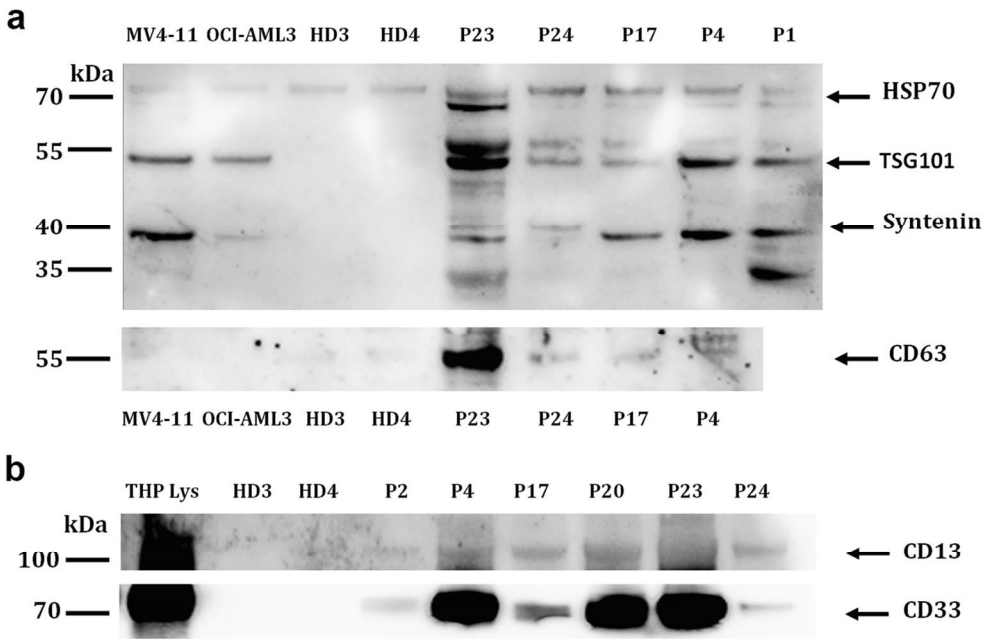

Fig. 2 Western blot analysis of EV-specific markers. **a** Western blot analysis of leukemia cell lines (MV4-11 and OCI-AML3 as positive control), healthy donors and AML patient samples for EV-specific antibodies. **b** Western blot analysis of THP1 lysate (positive control), healthy donors, and AML patient samples for myeloid-specific antibodies

(Fig. 4g). Healthy donor EV-DNA was also analyzed for comparison and it was found that healthy donor DNA reflected that of the after treatment samples (Fig. 4h). This result could reflect that the DNA fragment sizes are in some way affected by the AML disease state, or that the amount of DNA in healthy donor EVs or after treatment EVs is too low to detect these distinct groups. Furthermore, in the initial four patient samples where mutational status was analyzed using NGS analysis, the initially discovered AML-specific mutations were no longer detectable in the EV-dsDNA in two out of four patients after treatment (P1 and P4), suggesting that the decline in EV number after therapy is associated with a reduction in the number of cancer cells that contain AML-specific mutations (Table 1). Subsequently, sixteen more patient samples (P14-P29) were analyzed for specific AML mutations using GeneScan-based fragment-length analysis. These results supported the previous results obtained from NGS. AML-specific mutations were detectable in EV-DNA before treatment (except patient 15) but not after treatment, except in four patient samples (P17, P20, P21, and P29) where the mutations were still detectable in one after treatment sample (Table 1). In the majority of samples, the EV-dsDNA findings were corresponding to the gDNA mutational status provided by the AML diagnostic laboratory (Table 1). Additionally, in two patients (P2 and P15) no AML-specific mutations were detectable before treatment; therefore, it was obvious that after treatment, the mutations were still undetectable. Patient sample P3 had only single-nucleotide polymorphisms (SNPs) and no AML-specific mutations, logically serving as a positive control in our study. As expected, we observed that the SNPs were detectable in EV-dsDNA before and after treatment (Table 1), again suggesting that therapy in patients leads to a reduction of EVs released by leukemia cells without compromising the EVs released by healthy cells in blood circulation.

Discussion

In this study, we aimed to evaluate leukemia-derived EVs for their diagnostic importance, based on the fact that EVs derived from tumor cells or leukemia blasts illustrate specific protein, lipid, and nucleic acid signatures that represent the pathological state of the respective parental cells [25].

Firstly, we provided evidence that EVs were indeed present in our samples and some had a myeloid origin. Then, we showed that the number of EVs could perhaps be a useful diagnostic indicator, as EV numbers declined accumulatively after treatment. Secondly, after demonstrating that EVs in tumor patients contain dsDNA, we revealed a potential correlation between the mutational background and the dsDNA concentration before and after treatment. After testing our samples for their DNA quality, we wondered whether EV-dsDNA had the diagnostic potential to detect AML. In proof of principle experiments, we demonstrated that discovered somatic mutations were detectable in the EV-dsDNA of seventeen AML patients before treatment but not in EV-dsDNA after treatment, with an exception of three cases (P2, P3, and P15).

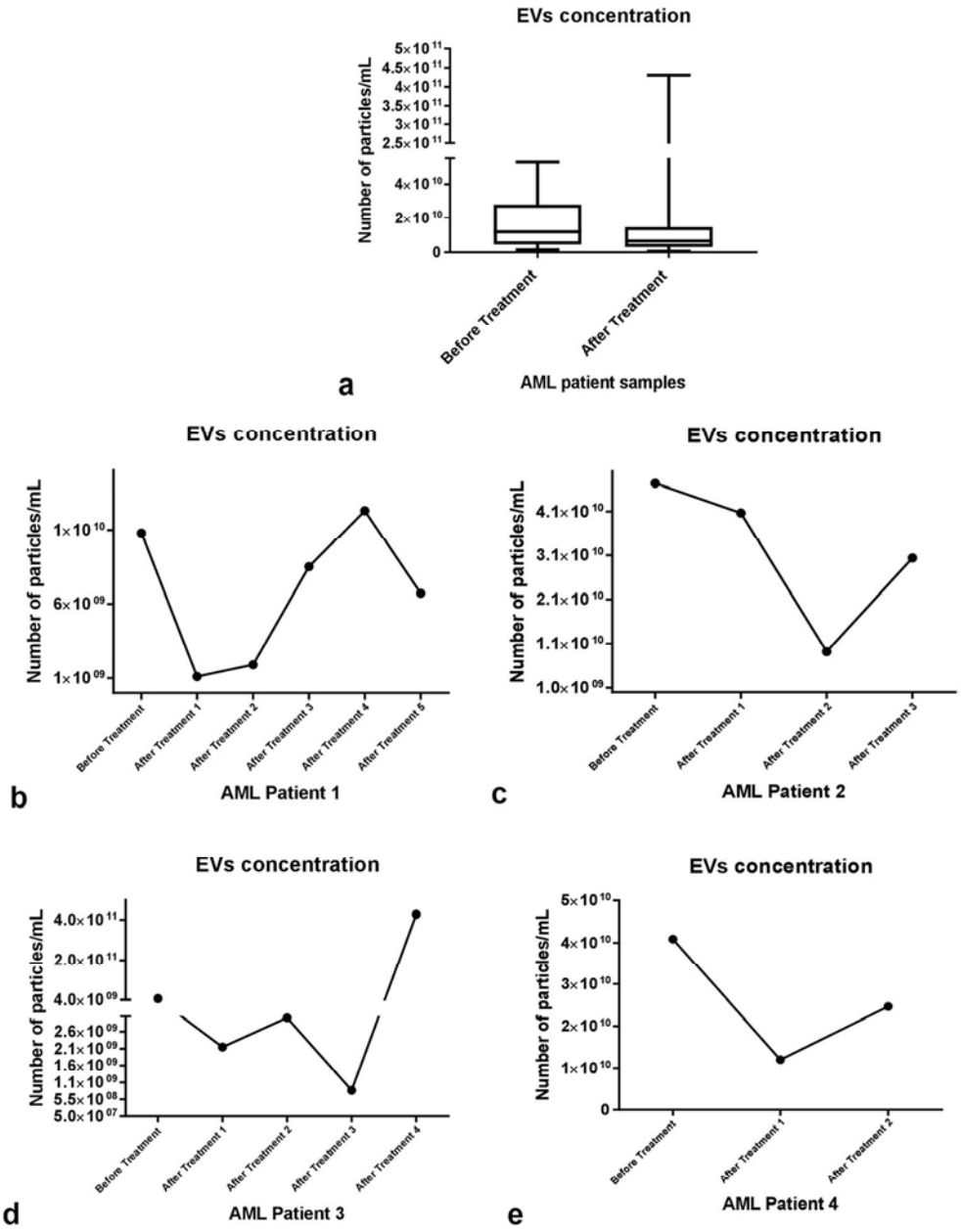

Fig. 3 Comparison of EVs before and after treatment. **a** Comparison of EV concentration in before and after treatment samples from 20 AML patients by NTA analysis. Higher concentration of EVs in before treatment samples was observed. **b**–**e** Individual monitoring of EV number using NTA. EVs isolated from the plasma of AML patients P1–P4 from before and after treatment

When considering the average EV concentration of all patients together, the observed overall reduction in EV concentration after treatment was expected, as the treatment should eliminate leukemia cells and, therefore, the number of leukemia-derived EVs in circulation. When considering the EV concentration results for each individual patient, fluctuation in the number of EVs after each treatment time point was observed which was not correlated to any other blood value such as the number of blasts. Consequently, the reason for these individual fluctuations are unclear; however, it could be related to normal myelopoiesis which may be a rich source of myeloid-derived EVs depending on regenerative activity and/or phases of cell destruction. Additionally, the result could be related to each person's individual response to the treatment, physical conditions, genetic background, etc. In future, to validate these results, it will be necessary to repeat this study using a large cohort of patients with well-chosen, age appropriate control subjects. In addition, the lifestyle factors which could influence the EV status of the participants in the study, e.g., circadian rhythm, exercise, nutrition, and stress, should be taken in to consideration at the time of the blood draw. Previously, it has been published that EVs released by cells of highly metastatic, malignant tumor cells contain high amounts of dsDNA [26]. Consequently, in this study, DNA isolated from EV fractions was detectable, and sometimes at an even higher concentration than the DNA of unfractionated

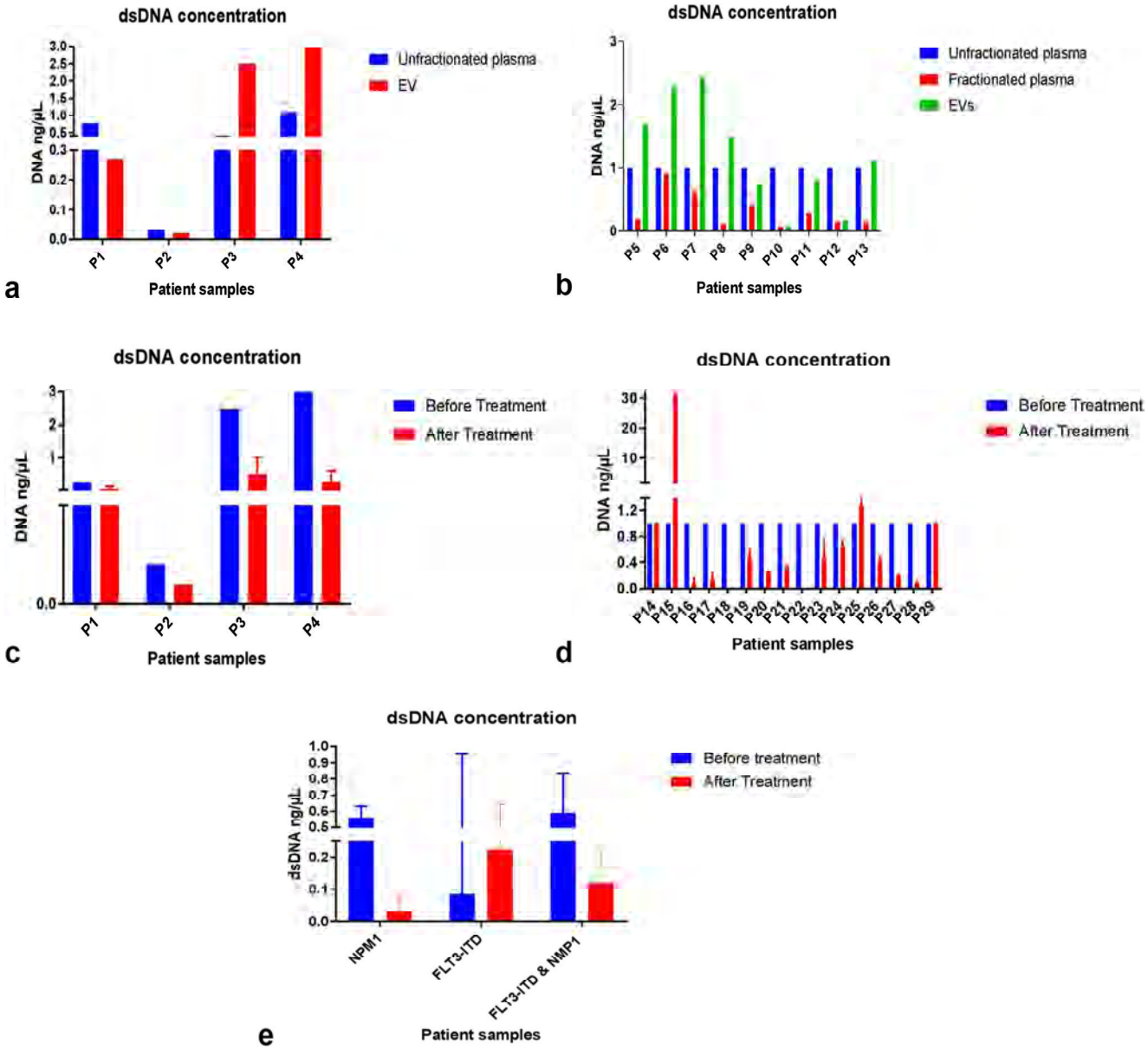

Fig. 4 Comparison of dsDNA from different plasma fractions and EV fraction in patient samples. **a** Comparison of dsDNA concentration that was extracted from unfractionated plasma and EV fractions of AML patients P1–P4. Qubit was used for the quantification of the samples. No specific trend was observed. **b** Comparison of dsDNA concentration that was extracted from unfractionated plasma, fractionated plasma, and EV fractions of AML patients P5-P13. dsDNA quantifluor was used for quantification and, again, no specific trend was observed. **c** Comparison of dsDNA concentration that was extracted from EV fractions of AML patients P1–P4 from before and after treatment. **d** Comparison of dsDNA concentration that was extracted from EV fractions of AML patients P14–P29 from before and after treatment. **e** Comparison of dsDNA concentration that was extracted from EV fractions of AML patients P14–P29 from before and after treatment, according to their mutational background. **f** Qualitative analysis of dsDNA of a patient sample before treatment. **g** Qualitative analysis of dsDNA of the same patient after treatment. **h** Qualitative analysis of dsDNA of a healthy donor sample

samples. EV-DNA and unfractionated DNA were sequenced to compare the mutational status with that of the corresponding patient gDNA that was recorded at primary diagnosis. As expected, the sequencing data revealed that the unfractionated plasma DNA and EV-DNA from the same individual patients had the exact same mutations, showing that, diagnostically speaking, the unfractionated DNA and the EV-DNA could complement each other. Routinely, after treatment, follow-up sequencing is performed using patient gDNA to analyze the mutational status of the patient. Therefore, in some cases, we were able to compare the mutational status between the gDNA and EV-DNA of patients after treatment. This analysis revealed that the EV-DNA and gDNA after treatment both showed the same absence of AML-specific mutations or the presence of SNPs in the majority of the samples, with mutational absence being presumably due to

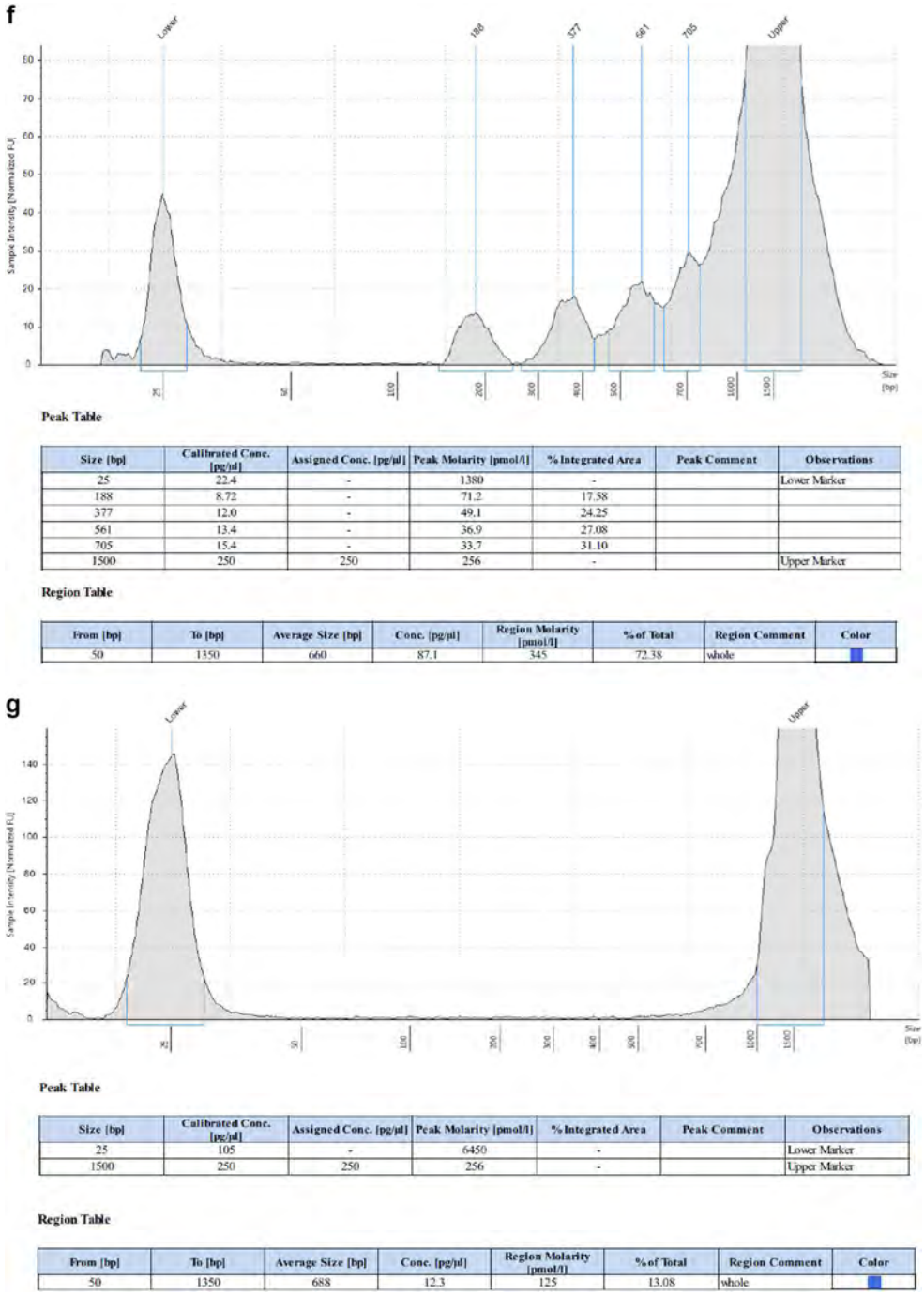

Fig. 4 continued.

the number of leukemic cells/EVs being reduced to such a low level that they no longer approached the detection threshold of the assay. Given that this method was mostly successful, in future, the plan would be to perform this assay with more sensitive sequencing methods, in order to further optimize the diagnostic potential of EV-DNA in AML. Due to the complexity of the disease, we are convinced that an elaborated understanding of clonal evolution in AML and an earlier detection of evolving AML sub-clones will help to improve diagnostic and therapeutic strategies. Accordingly, using the results from this current project and described future studies, the ultimate future aim would be to develop and establish a novel, highly sensitive EV-dsDNA-based analysis platform to serve as an additional approach to current leukemia diagnostic platforms, for obtaining additional/complementary information on leukemia cell populations. We believe that a diagnostic approach that combines multi-compartment blood

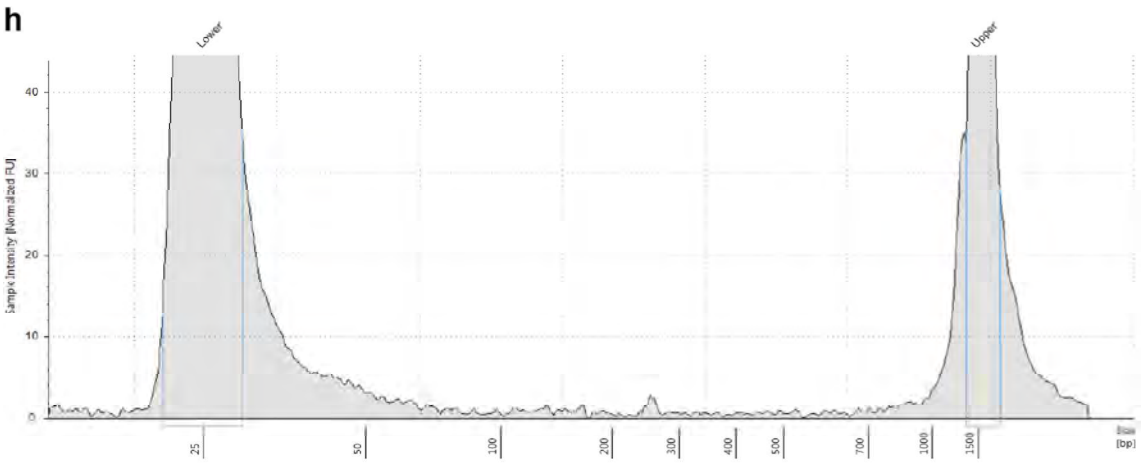

Peak Table

Size [bp]	Calibrated Conc. [pg/µl]	Assigned Conc. [pg/µl]	Peak Molarity [pmol/l]	% Integrated Area	Peak Comment	Observations
25	342	-	21000	-		Lower Marker
1500	250	250	256	-		Upper Marker

Region Table

From [bp]	To [bp]	Average Size [bp]	Conc. [pg/µl]	Region Molarity [pmol/l]	% of Total	Region Comment	Color
50	1350	752	30.8	248	30.78	whole	

Fig. 4 continued.

profiling in pediatric AML will prove to be superior to the current individual molecular diagnostic approaches that mainly focus on one class of diagnostic factors derived from leukemia blasts.

In conclusion, in this study, we demonstrated that AML-derived EVs contain DNA that reflects the mutational status of the cells of origin. To the best of our knowledge, this is the first study demonstrating the mutational analysis of EV-dsDNA in primary AML pediatric patient samples. Although these are very preliminary results, with further optimisation and additional large cohort studies this method could potentially enhance or

Table 3 Next generation sequencing analysis of four patient samples

Patient	Cancer type	Mutation in gDNA of AML cells	Primary leukemia cells	Unfractionated Plasma	EV-DNA
P1	AML-M1	NPM1 FLT3/TKD WT1 GATA2 ETV6 (SNP) ZRSR2(SNP)	NPM1 FLT3/TKD WT1 GATA2 ETV6 (SNP) ZRSR2(SNP)	NPM1 FLT3/TKD WT1 GATA2 ETV6 (SNP) ZRSR2(SNP)	NPM1 FLT3/TKD WT1 GATA2 ETV6 (SNP) ZRSR2(SNP)
P2	AML-M2	FLT3/ITD RAD21 KIT EZH2	FLT3/ITD RAD21 KIT EZH2	n.d n.d n.d n.d	n.d n.d n.d n.d
P3	AML-M3	GATA2 (SNP) NOTCH1 (SNP)	GATA2 (SNP) NOTCH1 (SNP)	GATA2 (SNP) NOTCH1 (SNP)	GATA2 (SNP) NOTCH1 (SNP)
P4	AML-M4	NRAS KIT (SNP) PHF6 (SNP)	NRAS KIT (SNP) PHF6 (SNP)	NRAS KIT (SNP) PHF6 (SNP)	NRAS KIT (SNP) PHF6 (SNP)

Next-generation sequencing analysis of known mutations was performed to investigate the diagnostic potential of DNA that was extracted from primary leukemia cells, unfractionated plasma, and EVs. The results were compared with the actual mutational status of the patients that was obtained from the already existing primary leukemia database in the AML-BFM lab. Four initial patient samples (P1–P4) before therapy were used for this analysis. For the sequencing, 50 ng or a maximum volume of 15 µL was used from each sample depending on their concentration. AML-specific mutations were detectable in all fractions of patient samples, except in patient 2. SNPs were present in all analyzed samples. Any "positive" or "negative" entries are mentioned by the name of the mutations or a note that the mutations were not detectable (n.d)

support classic AML detection methods that are currently used today, and will permit the development of new improved strategies for better diagnosis, prognosis, and therapy.

Acknowledgments We thank Dr. Verena Börger and Michel Bremer from the working group of Prof. Bernd Giebel, Institute of Transfusion Medicine, University Hospital of Essen, for introducing us to ultracentrifugation and NTA devices. We also thank Dr. Thomas Herold from the Institute of Pathology and Institute of Neuropathology for providing us access to devices for analyzing the quality of EV-DNA.

Authors' contribution Conception and design: BKT and EK; collection and assembly of data: EK, SS, KR, FK, CW, HJ, and BW; data analysis and interpretation: BKT, EK, HJ, MH, CW, and NVN; drafting of manuscript: BKT, EK, SS, and BG; manuscript writing: BKT, EK, and SS; final approval of manuscript: all co-authors.

Funding information The current study is supported by the José Carreras Leukemia Foundation grant DJCLS 18 R-2017 and Stiftung Universitätsmedizin Essen.

Compliance with ethical standards

Conflict of interest The authors declare that they have no conflicts of interest.

Informed consent Informed consent was obtained from all individual participants (or their parents) included in the study. Each patient was consented following institutional review board approval AML-BFM 2004 (3VCreutzig1).

Ethical approval All procedures performed in studies involving human participants were in accordance with the ethical standards of the institutional and/or national research committee and with the 1964 Helsinki declaration and its later amendments or comparable ethical standards.

Statement of welfare of animals This article does not contain any studies with animals performed by any of the authors.

References

1. Aziz H, Ping CY, Alias H, Ab Mutalib NS, Jamal R (2017) Gene mutations as emerging biomarkers and therapeutic targets for relapsed acute myeloid leukemia. Front Pharmacol 8:897. https://doi.org/10.3389/fphar.2017.00897
2. Grove CS, Vassiliou GS (2014) Acute myeloid leukaemia: a paradigm for the clonal evolution of cancer? Dis Model Mech 7(8):941–951. https://doi.org/10.1242/dmm.015974
3. Paietta E (2012) Minimal residual disease in acute myeloid leukemia: coming of age. Hematol Am Soc Hematol Educ Program 2012:35–42. https://doi.org/10.1182/asheducation-2012.1.35
4. Lane SW, Scadden DT, Gilliland DG (2009) The leukemic stem cell niche: current concepts and therapeutic opportunities. Blood 114(6):1150–1157. https://doi.org/10.1182/blood-2009-01-202606
5. Schepers K, Pietras EM, Reynaud D, Flach J, Binnewies M, Garg T, Wagers AJ, Hsiao EC, Passegue E (2013) Myeloproliferative neoplasia remodels the endosteal bone marrow niche into a self-reinforcing leukemic niche. Cell Stem Cell 13(3):285–299. https://doi.org/10.1016/j.stem.2013.06.009
6. Yanez-Mo M, Siljander PR, Andreu Z, Zavec AB, Borras FE, Buzas EI, Buzas K, Casal E, Cappello F, Carvalho J, Colas E, Cordeiro-da Silva A, Fais S, Falcon-Perez JM, Ghobrial IM, Giebel B, Gimona M, Graner M, Gursel I, Gursel M, Heegaard NH, Hendrix A, Kierulf P, Kokubun K, Kosanovic M, Kralj-Iglic V, Kramer-Albers EM, Laitinen S, Lasser C, Lener T, Ligeti E, Line A, Lipps G, Llorente A, Lotvall J, Mancek-Keber M, Marcilla A, Mittelbrunn M, Nazarenko I, Nolte-'t Hoen EN, Nyman TA, O'Driscoll L, Olivan M, Oliveira C, Pallinger E, Del Portillo HA, Reventos J, Rigau M, Rohde E, Sammar M, Sanchez-Madrid F, Santarem N, Schallmoser K, Ostenfeld MS, Stoorvogel W, Stukelj R, Van der Grein SG, Vasconcelos MH, Wauben MH, De Wever O (2015) Biological properties of extracellular vesicles and their physiological functions. J Extracell Vesicles 4:27066. https://doi.org/10.3402/jev.v4.27066
7. Deregibus MC, Cantaluppi V, Calogero R, Lo Iacono M, Tetta C, Biancone L, Bruno S, Bussolati B, Camussi G (2007) Endothelial progenitor cell derived microvesicles activate an angiogenic program in endothelial cells by a horizontal transfer of mRNA. Blood 110(7):2440–2448. https://doi.org/10.1182/blood-2007-03-078709
8. Ratajczak J, Miekus K, Kucia M, Zhang J, Reca R, Dvorak P, Ratajczak MZ (2006) Embryonic stem cell-derived microvesicles reprogram hematopoietic progenitors: evidence for horizontal transfer of mRNA and protein delivery. Leukemia 20(5):847–856. https://doi.org/10.1038/sj.leu.2404132
9. Valadi H, Ekstrom K, Bossios A, Sjostrand M, Lee JJ, Lotvall JO (2007) Exosome-mediated transfer of mRNAs and microRNAs is a novel mechanism of genetic exchange between cells. Nat Cell Biol 9(6):654–659. https://doi.org/10.1038/ncb1596
10. Castillo J, Bernard V, San Lucas FA, Allenson K, Capello M, Kim DU, Gascoyne P, Mulu FC, Stephens BM, Huang J, Wang H, Momin AA, Jacamo RO, Katz M, Wolff R, Javle M, Varadhachary G, Wistuba II, Hanash S, Maitra A, Alvarez H (2018) Surfaceome profiling enables isolation of cancer-specific exosomal cargo in liquid biopsies from pancreatic cancer patients. Ann Oncol 29(1):223–229. https://doi.org/10.1093/annonc/mdx542
11. Ludwig AK, Giebel B (2012) Exosomes: small vesicles participating in intercellular communication. Int J Biochem Cell Biol 44(1):11–15. https://doi.org/10.1016/j.biocel.2011.10.005
12. Fais S, O'Driscoll L, Borras FE, Buzas E, Camussi G, Cappello F, Carvalho J, Cordeiro da Silva A, Del Portillo H, El Andaloussi S, Ficko Trcek T, Furlan R, Hendrix A, Gursel I, Kralj-Iglic V, Kaeffer B, Kosanovic M, Lekka ME, Lipps G, Logozzi M, Marcilla A, Sammar M, Llorente A, Nazarenko I, Oliveira C, Pocsfalvi G, Rajendran L, Raposo G, Rohde E, Siljander P, van Niel G, Vasconcelos MH, Yanez-Mo M, Yliperttula ML, Zarovni N, Zavec AB, Giebel B (2016) Evidence-based clinical use of nanoscale extracellular vesicles in nanomedicine. ACS Nano 10(4):3886–3899. https://doi.org/10.1021/acsnano.5b08015
13. Thakur BK, Zhang H, Becker A, Matei I, Huang Y, Costa-Silva B, Zheng Y, Hoshino A, Brazier H, Xiang J, Williams C, Rodriguez-Barrueco R, Silva JM, Zhang W, Hearn S, Elemento O, Paknejad N, Manova-Todorova K, Welte K, Bromberg J, Peinado H, Lyden D (2014) Double-stranded DNA in exosomes: a novel biomarker in cancer detection. Cell Res 24(6):766–769. https://doi.org/10.1038/cr.2014.44
14. Hur JY, Kim HJ, Lee JS, Choi CM, Lee JC, Jung MK, Pack CG, Lee KY (2018) Extracellular vesicle-derived DNA for performing EGFR genotyping of NSCLC patients. Mol Cancer 17(1):15–16. https://doi.org/10.1186/s12943-018-0772-6
15. Yang S, Che SP, Kurywchak P, Tavormina JL, Gansmo LB, Correa de Sampaio P, Tachezy M, Bockhorn M, Gebauer F, Haltom AR, Melo SA, LeBleu VS, Kalluri R (2017) Detection of mutant KRAS and TP53 DNA in circulating exosomes from healthy individuals

and patients with pancreatic cancer. Cancer Biol Ther 18(3):158–165. https://doi.org/10.1080/15384047.2017.1281499
16. Wang L, Li Y, Guan X, Zhao J, Shen L, Liu J (2018) Exosomal double-stranded DNA as a biomarker for the diagnosis and preoperative assessment of pheochromocytoma and paraganglioma. Mol Cancer 17(1):128–126. https://doi.org/10.1186/s12943-018-0876-z
17. Kahlert C, Melo SA, Protopopov A, Tang J, Seth S, Koch M, Zhang J, Weitz J, Chin L, Futreal A, Kalluri R (2014) Identification of double-stranded genomic DNA spanning all chromosomes with mutated KRAS and p53 DNA in the serum exosomes of patients with pancreatic cancer. J Biol Chem 289(7):3869–3875. https://doi.org/10.1074/jbc.C113.532267
18. Svennerholm K, Rodsand P, Hellman U, Waldenstrom A, Lundholm M, Ahren D, Biber B, Ronquist G, Haney M (2016) DNA content in extracellular vesicles isolated from porcine coronary venous blood directly after myocardial ischemic preconditioning. PLoS One 11(7):e0159105. https://doi.org/10.1371/journal.pone.0159105
19. Vaidya M, Bacchus M, Sugaya K (2018) Differential sequences of exosomal NANOG DNA as a potential diagnostic cancer marker. PLoS One 13(5):e0197782. https://doi.org/10.1371/journal.pone.0197782
20. Hornick NI, Huan J, Doron B, Goloviznina NA, Lapidus J, Chang BH, Kurre P (2015) Serum exosome microRNA as a minimally-invasive early biomarker of AML. Sci Rep 5:11295. https://doi.org/10.1038/srep11295
21. Boyiadzis M, Whiteside TL (2016) Plasma-derived exosomes in acute myeloid leukemia for detection of minimal residual disease: are we ready? Expert Rev Mol Diagn 16(6):623–629. https://doi.org/10.1080/14737159.2016.1174578
22. Hong CS, Muller L, Whiteside TL, Boyiadzis M (2014) Plasma exosomes as markers of therapeutic response in patients with acute myeloid leukemia. Front Immunol 5:160. https://doi.org/10.3389/fimmu.2014.00160
23. Kunz F, Kontopoulou E, Reinhardt K, Soldierer M, Strachan S, Reinhardt D, Thakur BK (2019) Detection of AML-specific mutations in pediatric patient plasma using extracellular vesicle-derived RNA. Ann Hematol 98(3):595–603. https://doi.org/10.1007/s00277-019-03608-y
24. Fernando MR, Jiang C, Krzyzanowski GD, Ryan WL (2017) New evidence that a large proportion of human blood plasma cell-free DNA is localized in exosomes. PLoS One 12(8):e0183915. https://doi.org/10.1371/journal.pone.0183915
25. Whiteside TL (2016) Tumor-derived exosomes and their role in cancer progression. Adv Clin Chem 74:103–141. https://doi.org/10.1016/bs.acc.2015.12.005
26. Li X, Wang X (2017) The emerging roles and therapeutic potential of exosomes in epithelial ovarian cancer. Mol Cancer 16(1):92. https://doi.org/10.1186/s12943-017-0659-y

4. Diskussion

Mit einem Anteil von 15-20 % ist die akute myeloische Leukämie (AML) die zweithäufigste Leukämieform in der Kindheit (Downing & Shannon, 2002). Obwohl sich die Prognose von Kindern und Jugendlichen mit AML in den letzten Jahrzehnten deutlich verbessert hat - die langfristige Überlebensrate liegt bei bis zu 65 % (Kaspers & Zwaan, 2007) - erleidet die Mehrheit der Patienten nach drei bis fünf Jahren einen Rückfall (Paietta, 2012). Bislang mangelt es an einer Definition der Resterkrankung, die empfindlicher, spezifischer und objektiver als die klassische Morphologie ist, um einen personalisierten Ansatz für Behandlungsentscheidungen treffen zu können (Ossenkoppele & Schuurhuis, 2016). Die bislang standardisiert durchgeführten Assays und der aktuelle Wissensstand über die Entstehung und Ausprägung der AML können uns in Zukunft nützliche Werkzeuge in der Sensitivierung der Diagnostik werden. Die immer wieder erprobte Definition von prognostischen Gruppen zeigt auf, mit welchen Mutationen die Patienten am häufigsten ein Therapieversagen erleiden. Gerade diese prognostisch ungünstige Gruppe sollte in Zukunft eine verlässlichere und sensitivere Diagnostik erhalten, um frühzeitig einen möglichen Rückfall erkennen und behandeln zu können.

4.1 Erfolgreiche Mutationsdetektion in EV-RNA der Zelllinien

Extrazelluläre Vesikel werden von Zellen sowohl unter gesunden, als auch unter pathologischen Bedingungen freigesetzt. Durch ihre vielfältigen Beladungen, wie Nukleinsäuren und Proteine, gelten sie als entscheidend für die Entdeckung von Biomarkern für die klinische Diagnostik (Gurunathan, Kang, Jeyaraj, Qasim, & Kim, 2019). Beispielsweise werden EVs, die mit tumorspezifischen RNAs beladen sind, schon jetzt als Biomarker für die Krebsdiagnose in Studien verwendet (Gurunathan et al., 2019). Eine standardisierte Verwendung von EVs im klinischen Alltag ist derzeit allerdings noch nicht erprobt.

In der vorliegenden Arbeit wurden mit FLT3-ITD und NPM1 eine Typ-I und eine Typ-II Aberration für die Experimente der Zelllinien verwendet. Die Zelllinie MV4-11 trägt die FLT3-ITD und die Zelllinie OCI-AML3 trägt die NPM1 Mutation. Nach

Kultivierung der Zellen erfolgte die Gewinnung derer extrazellulärer Vesikel. Dies wurde via Ultrazentrifugation durchgeführt. Die gewonnen Proben wurden im Anschluss mittels Nanopartikel Tracking Analyse (NTA) auf die enthaltenen Vesikel untersucht. Nach der Quantifizierung der extrazellulären Vesikel erfolgte die Gewinnung der RNA. Eine durchgeführte RNA-Quantifizierung im Anschluss konnte das Vorliegen von RNA nachweisen und die gewonnene RNA-Menge bestimmen. Nach Sicherstellung der isolierten RNA wurde diese entweder mittels RealTime-PCR auf die NPM1 Mutation oder mittels Gene-Scan basierter Fragmentlängenanalyse auf die FLT3-ITD Mutation analysiert. Dabei bildete die jeweils für die Mutation negative Zelllinie die Negativkontrolle. Es zeigte sich, dass in den mutationspositiven Zellinien die Mutationen in der aus den Vesikeln isolierten RNA zu finden waren. Zusätzlich konnten in den den mutationsnegativen Zelllinien keine Signale ermittelt werden

4.2 RNA-Isolierung aus den EVs der pädiatrischen Plasmaproben

Im Anschluss an die erfolgreiche Testung in den Zelllinien führten wir die gleichen Verfahren mit den bereits beschriebenen Patientenproben der Kinderklinik durch. Diese enthielten wie auch die Zelllinien entweder eine Mutation mit NPM1, mit FLT3-ITD oder eine kombinierte Mutation aus beiden. Zunächst wurden auch aus den Patientenproben die extrazellulären Vesikel gewonnen. Es erfolgte eine Bestimmung der Anzahl und Größe der Vesikel. Hier wiesen die Patientengruppen große Unterschiede auf. Während in den Patientengruppen mit der NPM1 Mutation und der kombinierten Mutation die Anzahl der Vesikel nach der Behandlung geringer war als zum Zeitpunkt der Diagnosestellung, zeigten die Patienten mit der FLT3-ITD Mutation einen deutlichen Anstieg in den Verlaufskontrollen. Dies ließ sich zuvor auch in den Ergebnissen der Zelllinien widerspiegeln. Danach erfolgte die Isolierung der RNA mit anschließender Quantifizierung. Diese zeigte in den Konzentrationsspiegeln ebenfalls Unterschiede zwischen den Patientengruppen. Auch hier waren die RNA-Spiegel der Patienten mit FLT3-ITD Mutation in den Verlaufskontrollen höher als in den Proben zum Diagnosezeitpunkt, wohingegen in den Patienten mit NPM1 Mutation oder der kombinierten Mutation eine deutlich höhere RNA-Konzentration in den Proben zum Diagnosezeitpunkt zu finden war, was den Trend der Vesikelmenge bestätigt. Die

Unterschiede in den Partikelmengen könnten mit den verschiedenen Mutationen zusammenhängen oder jedoch mit den unterschiedlichen Patienten assoziiert sein, da unsere Berechnungen jeweils aus den Mittelwerten aller Patienten mit einer Mutation zum Zeitpunkt der Diagnose und addiert zu allen Zeitpunkten der Kontrolle berechnet wurden. Dennoch wäre eine Abhängigkeit der Partikelmenge von den unterschiedlichen Mutationen möglich. Die Unterschiede in der RNA-Konzentration lässt sich schließlich mit der Menge an Partikeln erklären. In den Proben mit vielen Partikeln fand sich entsprechend viel RNA.

4.3 Analyse der EV-RNA der Patientenproben

Bislang gibt es nur wenige Studien, die sich mit dem Mutationsstatus der DNA oder RNA von extrazellulären Vesikeln befassen. Die Studie von Figueroa et al. von 2017 zeigt das Vorhandensein von Tumor-spezifischen Mutationen des Glioblastoms in der RNA von extrazellulären Vesikeln, die aus Liquorpunktionen gewonnen wurden. (Figueroa et al., 2017).
Die Analyse der AML-Plasmaproben im Hinblick auf die Mutationen zeigte, dass die NPM1-Mutation in 7 Patienten zum Zeitpunkt der Diagnose zu finden war. Lediglich in 2 Patientenproben war es nicht möglich, die Mutation zu detektieren. In den Patientenproben mit FLT3-ITD Mutation hingegen war es möglich, die Mutation in allen Initialproben zu detektieren. Dies spricht für eine höhere Sensitivität unter Verwendung der Gene-Scan basierten Fragmentlängenanalyse im Vergleich zu der durchgeführten RealTime-PCR.
Dennoch waren die Mutationen in den Proben nach Therapiebeginn nicht länger detektierbar und deren Fehlen nach der Behandlung stand nicht immer in Korrelation zu den Ergebnissen der genomischen DNA-Analyse, die routinemäßig nach jeder Probenentnahme in dem diagnostischen AML-Labor der AML-BFM-Studiengruppe durchgeführt wird. An dieser Stelle wird deutlich, dass gerade in den Folgekontrollen der Patienten die gewünschte Funktion der Vesikel zur Erkennung der Resterkrankung bislang ausbleibt. Ursachen könnten unter anderem sein, dass die in den EVs vorliegende Menge an genetischem Material sehr begrenzt ist. In den Proben zum Diagnosezeitpunkt ist die Blastenzahl der Patienten überdurchschnittlich hoch, was

auch die Menge der EVs beeinflusst. Nach Therapiebeginn sinkt die Anzahl der Blasten jedoch deutlich und es werden fortan auch weniger Vesikel produziert. Eine andere Vermutung wäre die Diversität der einzelnen Vesikel. Denkbar wären verschiedene DNA- und RNA-Inhalte, die nicht alle die Information der vorliegenden Mutationen enthalten, was die Detektion deutlich erschweren würde.

4.4 Quantifizierung der EVs aus weiteren Patientenproben

In den Versuchsreihen dienten 5 Kontrollplasmaproben von gesunden Spendern als Referenz. Hiermit sollte eine Aussage darüber getroffen werden, wie die gesunden Kontrollen im Vergleich zu den Patientenproben in den Assays reagieren, bzw. wo quantitative Unterschiede zum Beispiel in Bezug auf die Partikelmenge liegen. Die Patienten wiesen über den Therapieverlauf fluktuierende Level an Vesikeln auf, jedoch war in jedem von ihnen die Menge der Vesikel vor Therapiebeginn am höchsten.

Es folgten weitere Assays zur Quantifizierung. Zum einen wurde ein Bicinchoninsäure-Assay (BCA) durchgeführt, eine Methode zur qunatitativen Proteinbestimmung, das eine Korrelation zwischen der Partikelmenge und der vorhandenen Proteinmenge aufwies. Zum anderen wurden Western Blots mit verschiedenen Antikörpern durchgeführt, die spezifisch für die Detektion von EVs oder myeloischen Zellen verwendet werden. Es zeigte sich, dass alle Patientenproben positiv auf die verwendeten Marker reagierten, wohingegen die gesunden Kontrollen nicht alle Signale bei den EV-spezifischen Markern und keine Signale bei Marken für myeloische Zellen zeigten. Dies könnte daran begründet sein, dass die Anzahl der Vesikel bei gesunden Spendern im Vergleich zu der Anzahl der Vesikel in den Patientenproben signifikant niedriger war. Die gewonnene Menge an Proteinen ist ebenfalls deutlich geringer bei den gesunden Kontrollen, im Vergleich zu den Patienten.

4.5 Analyse der EV-DNA auf Mutationsstatus

Nach den EV-Quantifizierungsschritten wurden 20 der 29 Patienten des Kollektivs für die weiteren Versuche ausgewählt, aus deren Proben nun die dsDNA gewonnen und im Anschluss quatifiziert wurde. Es zeigte sich, dass in den meisten Patientenproben die

dsDNA-Spiegel vor Therapiebeginn höher waren als in den Verlaufsproben. Allein die Patienten mit der FLT3-ITD Mutation wiesen erhöhte dsDNA-Spiegel in den Kontrollproben auf, was den bereits in der RNA aufgezeigten Trend für diese Mutation bestätigt. Zur weiteren Charakterisierung der DNA wurden 4 Proben mittels Bioanalysierer untersucht. Es zeigte sich, dass sich in den EVs zum Zeitpunkt der Diagnose vier Fragmentgrößen nachweisen ließen, in den Proben nach der Behandlung jedoch nur drei. Die Kontrollproben der gesunden Spender zeigten die gleichen Ergebnisse, wie die Proben nach der Therapie. Ursächlich könnte zum einen eine mögliche Beeinflussung der AML in Bezug auf die DNA sein. Zum anderen könnte eine unzureichende Menge an Material bei den gesunden Kontrollen sowie den Patientenproben nach der Therapie dafür verantwortlich sein, dass die zusätzliche Fragmentgröße nicht detektierbar war.

Im Anschluss wurden 4 Patienten ausgewählt und via Next Generation Sequencing (NGS) sequenziert. Es zeigte sich, dass sich in 3 Patienten dieselben Mutationen in der EV-DNA finden ließen, die auch in der genomischen DNA (gDNA) der Initialproben gefunden wurden. Bei einem Patienten war es hingegen nicht möglich, die in der gDNA gezeigten Mutationen in der EV-DNA zu detektieren.

Weitere 16 Patienten wurden mittels Gene-Scan basierter Fragmentlängenanalyse hinsichtlich ihrer Mutationen untersucht. Die Ergebnisse bestärken die zuvor bereits mit der EV-RNA durchgeführten Analysen. Auch in diesem Assay zeigten sich die in der gDNA bereits gefundenen Mutationen in der EV-DNA der Initialproben. Lediglich in einer Probe war keine Mutation detektierbar. In vier der 16 gemessenen Proben war es zudem möglich, in einer weiteren Probe zu einem Kontrollzeitpunkt die entsprechende Mutation zu detektieren. Bei den übrigen Patienten geling dies leider nur zum Zeitpunkt der Diagnose.

4.6 Fazit

Ziel dieser Arbeit war es, die Bedeutung und klinische Verwendung von extrazellulären Vesikeln in der pädiatrischen AML zu erläutern.

In dieser Studie konnten wir zeigen, dass die aus den extrazellulären Vesikeln der Patientenproben isolierte DNA und RNA den Mutationsstatus der Ursprungszellen nachweisen. Als Vergleich diente uns die in der Routine durchgeführte gDNA-Analyse.

Unser derzeitiger Ansatz zeigt bereits erste Ergebnisse, jedoch sind diese gerade im Hinblick auf die Sensitivität eingeschränkt. Obwohl es uns gelang, die Mutationen bei fast allen Patienten zum Zeitpunkt der Diagnose zu detektieren, war es nur selten zum Zeitpunkt nach der Therapie möglich. Im Vergleich war auch die Sensitivität in der Studie von Figueroa et al. 2017 mit 61 % relativ gering. Es war Ihnen möglich, die Mutation in 14 der 23 positiv vorgetesteten Patienten zu detektieren, zudem auch in einem negativ getesteten Patienten, was aufzeigt, dass nicht nur in unserer Studie die Sensitivität in Bezug auf die Arbeit mit genetischem Material von extrazellulären Vesikeln eine Hürde ist, die es zu überwinden gilt.

Jedoch ist gerade nach der Therapie der entscheidende Zeitraum, in welchem eine bessere Erkennung und Detektion von möglichen verbleibenden Tumorzellen gefordert ist. Eine gezieltere Materialgewinnung mit anschließender Vervielfachung wird notwendig sein, um auch in den Proben nach der Therapie Ergebnisse nachweisen zu können.

Wie alle neuen Ansätze erfordert auch dieser eine Optimierungsphase, bevor er in der klinischen Routine zum Einsatz kommen kann. Essenziell wäre hier eine Studie mit deutlich größerer Kohorte und eine bessere Methode, um gezielt AML-spezifische EVs zu isolieren. Derzeit gibt es bereits erste Ansätze zur Sortierung der einzelnen EV-Populationen, zum Beispiel via NanoFACS (Morales-Kastresana et al., 2019), jedoch wird es noch Zeit brauchen, um die Methoden gezielt für klinische Assays nutzen zu können.

Dennoch bietet unsere Studie einen möglichen Startpunkt, der den klinischen Nutzen von extrazellulären Vesikeln aufzeigen konnte, um vielleicht zukünftig bisherige AML-

Nachweismethoden zu unterstützen und zudem zur Entwicklung verbesserter Strategien für die Diagnose, Prognose und Therapie der AML beizutragen (Kunz et al., 2019).

5. Zusammenfassung

In der vorliegenden wissenschaftlichen Arbeit wurde die klinische Verwendung und der Nutzen von extrazellulären Vesikeln (EV) in der pädiatrischen akuten myeloischen Leukämie (AML) untersucht. Dafür wurden 166 Plasmaproben von 45 Patienten mit bekannter AML aus der Biobank der Kinderklinik III der Universitätsklinik Essen verwendet, um die darin enthaltenen extrazellulären Vesikel zu extrahieren und analysieren, um eine alternative Nachweismethode für AML-spezifische Mutationen zu etablieren. Die Plasmaproben wurden jeweils zum Zeitpunkt der Diagnose und zu weiteren Verlaufskontrollen entnommen. Im Vorfeld erfolgte Experimente auf Zellebene wurden mit zwei klassischen AML-Zelllinien durchgeführt. Nach Kultivierung erfolgte die Gewinnung der extrazellulären Vesikel mittels Ultrazentrifugation. Anschließend wurde aus diesen die RNA gewonnen und mittels RealTime-PCR oder GeneScan basierter Fragmentlängenanalyse auf mögliche Mutationen untersucht. Hierbei zeigte sich, dass nur die für die Mutation positive Zelllinie Signale in den Assays zeigte. Im Anschluss wurden die extrazellulären Vesikel der Patientenproben gewonnen. Aus den EVs von insgesamt 29 ausgewählten Patienten wurde nun entweder die DNA und / oder RNA gewonnen und quantifiziert. Die RNA-Analyse der Mutationen zeigte, dass die NPM1-Mutation in sieben Patienten zum Zeitpunkt der Diagnose zu finden war. Lediglich in zwei Patientenproben war dies nicht möglich. In den Patientenproben mit FLT3-ITD Mutation war es möglich, die Mutation in allen Initialproben zu detektieren. Dennoch waren die Mutationen in den Proben nach Therapiebeginn nicht länger detektierbar, was nicht immer in Korrelation mit den Ergebnissen der routinemäßig durchgeführten genomischen DNA-Analyse stand, die in unserem diagnostischen AML-Labor durchgeführt wird. Weitere 16 Patienten wurden mittels Gene-Scan basierter Fragmentlängenanalyse hinsichtlich ihrer Mutationen in der EV-DNA untersucht. Auch in diesem Assay zeigten sich die in der gDNA bereits gefundenen Mutationen in der EV-DNA der Initialproben. Lediglich in einer Probe war keine Mutation detektierbar. In vier der 16 gemessenen Proben war es zudem möglich, in einer Folgeprobe die entsprechende Mutation zu detektieren. Zusammenfassend lässt sich sagen, dass es uns gelang, in fast allen Proben zur Diagnosestellung die Mutation in der EV-RNA bzw. EV-DNA zu finden, jedoch nicht nach Therapiebeginn.

Summary

The aim of this study was to evaluate the role and clinical benefit of extracellular vesicles (EV) in pediatric acute myeloid leukemia (AML). For this purpose, 166 plasma samples from 45 patients with known AML from the Biobank of the Children's Hospital III of the University Hospital Essen were used to extract and analyse the extracellular vesicles contained therein to establish an alternative detection method for AML-specific mutations. The collected plasma samples were each taken at the time of diagnosis and for further follow-up. Preliminary cell-level experiments were performed using two classical AML cell lines. After cultivation, the extracellular vesicles were obtained by ultracentrifugation. Subsequently, RNA was extracted from these and analysed for possible mutations using RealTime PCR or GeneScan-based fragment length analysis. There, signals in the assays were only observed in the cell line positive for the mutation. Subsequently, the extracellular vesicles of the patient samples were also obtained. From the EVs of a total of 29 selected patients, either the DNA and / or the RNA was now obtained and quantified. RNA analysis of the mutations revealed that the NPM1 mutation was found in seven patients at the time of diagnosis, whereas this was not possible in two patient samples. In the patient samples with FLT3-ITD mutation, it was possible to detect the mutation in all initial samples. However, the initial mutations were no longer detectable in the samples after treatment initiation which was not always in correlation with the results of routine genomic DNA analysis performed in our diagnostic AML laboratory. An additional 16 patients were evaluated for their EV DNA mutations by gene scan-based fragment length analysis. Also, in this assay, the mutations already found in the gDNA showed up in the EV DNA of the initial samples. Only in one sample, no mutation was detectable. In four of the 16 samples measured, it was also possible to detect the corresponding mutation in a follow-up sample. In summary, we succeeded in finding the mutation in EV RNA and EV DNA in almost all samples at the time of diagnosis, but not in the follow-up controls after the start of therapy.

6. Literaturverzeichnis

1. Abels, E. R., & Breakefield, X. O. (2016). Introduction to Extracellular Vesicles: Biogenesis, RNA Cargo Selection, Content, Release, and Uptake. *Cell Mol Neurobiol, 36*(3), 301-312
2. Akers, J. C., Gonda, D., Kim, R., Carter, B. S., & Chen, C. C. (2013). Biogenesis of extracellular vesicles (EV): exosomes, microvesicles, retrovirus-like vesicles, and apoptotic bodies. *J Neurooncol, 113*(1), 1-11.
3. Arber, D. A., Orazi, A., Hasserjian, R., Thiele, J., Borowitz, M. J., Le Beau, M. M., Bloomfield, C. D., Cazzola, M., Vardiman, J. W. (2016). The 2016 revision to the World Health Organization classification of myeloid neoplasms and acute leukemia. *Blood, 127*(20), 2391-2405.
4. Aziz, H., Ping, C. Y., Alias, H., Ab Mutalib, N. S., & Jamal, R. (2017). Gene Mutations as Emerging Biomarkers and Therapeutic Targets for Relapsed Acute Myeloid Leukemia. *Front Pharmacol, 8*, 897.
5. Bach, D. H., Hong, J. Y., Park, H. J., & Lee, S. K. (2017). The role of exosomes and miRNAs in drug-resistance of cancer cells. *Int J Cancer, 141*(2), 220-230.
6. Balgobind, B. V., Hollink, I. H., Arentsen-Peters, S. T., Zimmermann, M., Harbott, J., Beverloo, H. B., von Bergh, A. R. M., Cloos, J., Kaspers G. J. L., de Haas, V., Zemanova, Z., Stary J., Cayuela, J.-M., Baruchel, A., Creutzig, U., Reinhardt, D., Pieters, R., Zwaan, C. M., van den Heuvel-Eibrink, M. M. (2011). Integrative analysis of type-I and type-II aberrations underscores the genetic heterogeneity of pediatric acute myeloid leukemia. *Haematologica, 96*(10), 1478-1487.
7. Batista, I. A., & Melo, S. A. (2019). Exosomes and the Future of Immunotherapy in Pancreatic Cancer. *Int J Mol Sci, 20*(3). doi:10.3390/ijms20030567
8. Becker, A., Thakur, B. K., Weiss, J. M., Kim, H. S., Peinado, H., & Lyden, D. (2016). Extracellular Vesicles in Cancer: Cell-to-Cell Mediators of Metastasis. *Cancer Cell, 30*(6), 836-848.
9. Bennett, J. M., Catovsky, D., Daniel, M. T., Flandrin, G., Galton, D. A., Gralnick, H. R., & Sultan, C. (1976). Proposals for the classification of the acute leukaemias. French-American-British (FAB) co-operative group. *Br J Haematol, 33*(4), 451-458.
10. Bhatnagar, N., Nizery, L., Tunstall, O., Vyas, P., & Roberts, I. (2016). Transient Abnormal Myelopoiesis and AML in Down Syndrome: an Update. *Curr Hematol Malig Rep, 11*(5), 333-341.
11. Borges, F. T., Reis, L. A., & Schor, N. (2013). Extracellular vesicles: structure, function, and potential clinical uses in renal diseases. *Braz J Med Biol Res, 46*(10), 824-830.
12. Boyiadzis, M., & Whiteside, T. L. (2016). Plasma-derived exosomes in acute myeloid leukemia for detection of minimal residual disease: are we ready? *Expert Rev Mol Diagn, 16*(6), 623-629.
13. Caivano, A., La Rocca, F., Simeon, V., Girasole, M., Dinarelli, S., Laurenzana, I., De Stradis, A., De Luca, L., Trino, S., Traficante, A., D'Arena, G., Mansueto, G., Villani, O., Pietrantuono, G., Laurenti, L., Del Vecchio, L., Musto, P. (2017). MicroRNA-155 in serum-derived extracellular vesicles as a potential biomarker for hematologic malignancies - a short report. *Cell Oncol (Dordr), 40*(1), 97-103.

14. Caivano, A., Laurenzana, I., De Luca, L., La Rocca, F., Simeon, V., Trino, S., D'Auria, F., Traficante, A., Maietti, M., Izzo, T., D'Arena, G., Mansueto, G., Pietrantouno, G., Laurenti, L., Musto, P., Del Vecchio, L. (2015). High serum levels of extracellular vesicles expressing malignancy-related markers are released in patients with various types of hematological neoplastic disorders. *Tumour Biol, 36*(12), 9739-9752.
15. Castillo, J., Bernard, V., San Lucas, F. A., Allenson, K., Capello, M., Kim, D. U., Gascoyne, P., Mulu, F. C., Stephens, B. M., Huang, J., Wang, H., Momin, A. A., Jacamo, R. O., Katz, M., Wolff, R., Javle, M., Varadhachary, G., Wistuba, I. I., Hanash, S., Maitra, A., Alvarez, H. (2018). Surfaceome profiling enables isolation of cancer-specific exosomal cargo in liquid biopsies from pancreatic cancer patients. *Ann Oncol, 29*(1), 223-229.
16. Choi, D. S., Kim, D. K., Kim, Y. K., & Gho, Y. S. (2015). Proteomics of extracellular vesicles: Exosomes and ectosomes. *Mass Spectrom Rev, 34*(4), 474-490.
17. Clayton, A., Mitchell, J. P., Court, J., Linnane, S., Mason, M. D., & Tabi, Z. (2008). Human tumor-derived exosomes down-modulate NKG2D expression. *J Immunol, 180*(11), 7249-7258. doi:10.4049/jimmunol.180.11.7249
18. Colombo, E., Marine, J. C., Danovi, D., Falini, B., & Pelicci, P. G. (2002). Nucleophosmin regulates the stability and transcriptional activity of p53. *Nat Cell Biol, 4*(7), 529-533.
19. Creutzig, U., Zimmermann, M., Reinhardt, D., Rasche, M., von Neuhoff, C., Alpermann, T., Dworzak, M., Perglerová, K., Zemanova, Z., Tchinda, J., Bradtke, J., Thiede, C., Haferlach, C. (2016). Changes in cytogenetics and molecular genetics in acute myeloid leukemia from childhood to adult age groups. *Cancer, 122*(24), 3821-3830.
20. Deregibus, M. C., Cantaluppi, V., Calogero, R., Lo Iacono, M., Tetta, C., Biancone, L., Bruno, S., Bussolati, B., Camussi, G. (2007). Endothelial progenitor cell derived microvesicles activate an angiogenic program in endothelial cells by a horizontal transfer of mRNA. *Blood, 110*(7), 2440-2448.
21. Fais, S., O'Driscoll, L., Borras, F. E., Buzas, E., Camussi, G., Cappello, F., Carvalho, J., Cordeiro da Silva, A., Del Portillo, H., El Andaloussi, S., Ficko Trček, T., Furlan, R., Hendrix, A., Gursel, I., Kralj-Iglic, V., Kaeffer, B., Kosanovic, M., Lekka, M. E., Lipps, G., Logozzi, M., Marcilla, A., Sammaer, M., Llorente, A., Nazarenko, I., Oliveira, C., Pocsfalvi, G., Rajendran, L., Raposo, G., Rohde, E., Siljander, P., van Niel, G., Vasconcelos, M. H., Yáñez-Mó, M., Yliperttula, M. L., Zarovni, N., Zavec, A. B., Giebel, B. (2016). Evidence-Based Clinical Use of Nanoscale Extracellular Vesicles in Nanomedicine. *ACS Nano, 10*(4), 3886-3899.
22. Fernando, M. R., Jiang, C., Krzyzanowski, G. D., & Ryan, W. L. (2017). New evidence that a large proportion of human blood plasma cell-free DNA is localized in exosomes. *PLoS One, 12*(8), e0183915.
23. Figueroa, J. M., Skog, J., Akers, J., Li, H., Komotar, R., Jensen, R., Ringel, F., Yang, I., Kalkanis, S., Thompson, R., LoGuidice, L., Berghoff, E., Parsa, A., Liau, L., Curry, W., Cahill, D., Bettegowda, C., Lang, F. F., Chiocca, E. A., Henson, J., Kim, R., Breakefield, X., Chen, C., Messer, K., Hochberg, F., Carter, B. S. (2017). Detection of wild-type EGFR amplification and EGFRvIII mutation in CSF-

derived extracellular vesicles of glioblastoma patients. *Neuro Oncol, 19*(11), 1494-1502.
24. Gould, S. J., & Raposo, G. (2013). As we wait: coping with an imperfect nomenclature for extracellular vesicles. *J Extracell Vesicles, 2*.
25. Grove, C. S., & Vassiliou, G. S. (2014). Acute myeloid leukaemia: a paradigm for the clonal evolution of cancer? *Dis Model Mech, 7*(8), 941-951.
26. Gurunathan, S., Kang, M. H., Jeyaraj, M., Qasim, M., & Kim, J. H. (2019). Review of the Isolation, Characterization, Biological Function, and Multifarious Therapeutic Approaches of Exosomes. *Cells, 8*(4).
27. Heath, E. M., Chan, S. M., Minden, M. D., Murphy, T., Shlush, L. I., & Schimmer, A. D. (2017). Biological and clinical consequences of NPM1 mutations in AML. *Leukemia, 31*(4), 798-807.
28. Hingorani, K., Szebeni, A., & Olson, M. O. (2000). Mapping the functional domains of nucleolar protein B23. *J Biol Chem, 275*(32), 24451-24457.
29. Hong, C. S., Muller, L., Whiteside, T. L., & Boyiadzis, M. (2014). Plasma exosomes as markers of therapeutic response in patients with acute myeloid leukemia. *Front Immunol, 5*, 160.
30. Hornick, N. I., Huan, J., Doron, B., Goloviznina, N. A., Lapidus, J., Chang, B. H., & Kurre, P. (2015). Serum Exosome MicroRNA as a Minimally-Invasive Early Biomarker of AML. *Sci Rep, 5*, 11295.
31. Huan, J., Hornick, N. I., Shurtleff, M. J., Skinner, A. M., Goloviznina, N. A., Roberts, C. T., Jr., & Kurre, P. (2013). RNA trafficking by acute myelogenous leukemia exosomes. *Cancer Res, 73*(2), 918-929.
32. Hur, J. Y., Kim, H. J., Lee, J. S., Choi, C. M., Lee, J. C., Jung, M. K., Pack, C. G., Lee, K. Y. (2018). Extracellular vesicle-derived DNA for performing EGFR genotyping of NSCLC patients. *Mol Cancer, 17*(1), 15.
33. Kahlert, C., Melo, S. A., Protopopov, A., Tang, J., Seth, S., Koch, M., Zhang, J., Weitz, J., Chin, L., Futreal, A., Kalluri, R. (2014). Identification of double-stranded genomic DNA spanning all chromosomes with mutated KRAS and p53 DNA in the serum exosomes of patients with pancreatic cancer. *J Biol Chem, 289*(7), 3869-3875.
34. Keller, S., Ridinger, J., Rupp, A. K., Janssen, J. W., & Altevogt, P. (2011). Body fluid derived exosomes as a novel template for clinical diagnostics. *J Transl Med, 9*, 86.
35. Kiyoi, H., Kawashima, N., & Ishikawa, Y. (2020). FLT3 mutations in acute myeloid leukemia: Therapeutic paradigm beyond inhibitor development. *Cancer Sci, 111*(2), 312-322.
36. Kunz, F., Kontopoulou, E., Reinhardt, K., Soldierer, M., Strachan, S., Reinhardt, D., & Thakur, B. K. (2019). Detection of AML-specific mutations in pediatric patient plasma using extracellular vesicle-derived RNA. *Ann Hematol, 98*(3), 595-603.
37. Lagunas-Rangel, F. A., & Chávez-Valencia, V. (2017). FLT3-ITD and its current role in acute myeloid leukaemia. *Med Oncol, 34*(6), 114.
38. Lane, S. W., Scadden, D. T., & Gilliland, D. G. (2009). The leukemic stem cell niche: current concepts and therapeutic opportunities. *Blood, 114*(6), 1150-1157.
39. Li, X., & Wang, X. (2017). The emerging roles and therapeutic potential of exosomes in epithelial ovarian cancer. *Mol Cancer, 16*(1), 92.

40. Lonetti, A., Pession, A., & Masetti, R. (2019). Targeted Therapies for Pediatric AML: Gaps and Perspective. *Front Pediatr, 7*, 463. doi:10.3389/fped.2019.00463
41. Ludwig, A. K., & Giebel, B. (2012). Exosomes: small vesicles participating in intercellular communication. *Int J Biochem Cell Biol, 44*(1), 11-15.
42. Morales-Kastresana, A., Musich, T. A., Welsh, J. A., Telford, W., Demberg, T., Wood, J. C. S., Bigos, M., Ross, C. D., Kachynski, A., Dean, A., Felton, E. J., Van Dyke, J., Tigges, J., Toxavidis, V., Parks, D. R., Overton, W. R., Kesarwala, A. H., Freeman, G. J., Rosner, A., Perfetto, S. P., Pasquet, L., Terabe, M., McKinnon, K., Kapoor, V., Trepel, J. B., Puri, A., Kobayashi, H., Yung, B., Chen, X., Guion, P., Choyke, P., Knox, S. J., Ghiran, I., Robert-Guroff, M., Berzofsky, J. A., Jones, J. C. (2019). High-fidelity detection and sorting of nanoscale vesicles in viral disease and cancer. *J Extracell Vesicles, 8*(1), 1597603.
43. Nakao, M., Yokota, S., Iwai, T., Kaneko, H., Horiike, S., Kashima, K., Sonoda, Y., Fujimoto, T., Misawa, S. (1996). Internal tandem duplication of the flt3 gene found in acute myeloid leukemia. *Leukemia, 10*(12), 1911-1918.
44. Nerlov, C. (2007). The C/EBP family of transcription factors: a paradigm for interaction between gene expression and proliferation control. *Trends Cell Biol, 17*(7), 318-324.
45. Okuda, M., Horn, H. F., Tarapore, P., Tokuyama, Y., Smulian, A. G., Chan, P. K., Knudsen, E. S., Hofmann, I. A., Snyder, J. D., Bove, K. E., Fukasawa, K. (2000). Nucleophosmin/B23 is a target of CDK2/cyclin E in centrosome duplication. *Cell, 103*(1), 127-140.
46. Ossenkoppele, G., & Schuurhuis, G. J. (2016). MRD in AML: does it already guide therapy decision-making? *Hematology Am Soc Hematol Educ Program, 2016*(1), 356-365.
47. Paietta, E. (2012). Minimal residual disease in acute myeloid leukemia: coming of age. *Hematology Am Soc Hematol Educ Program, 2012*, 35-42.
48. Pando, A., Reagan, J. L., Quesenberry, P., & Fast, L. D. (2018). Extracellular vesicles in leukemia. *Leuk Res, 64*, 52-60.
49. Peinado, H., Alečković, M., Lavotshkin, S., Matei, I., Costa-Silva, B., Moreno-Bueno, G., Hergueta-Redondo, M., Williams, C., García-Santos, G., Ghajar, C., Nitadori-Hoshina, A., Hoffman, C., Badal, K., Garcia, B. A., Callahan, M. K., Yuan, J., Martins, V. R., Skog, J., Kaplan, R. N., Brady, M. S., Wolchok, J. D., Chapman, P. B., Kang, Y., Bromberg, J., Lyden, D. (2012). Melanoma exosomes educate bone marrow progenitor cells toward a pro-metastatic phenotype through MET. *Nat Med, 18*(6), 883-891.
50. Raposo, G., & Stoorvogel, W. (2013). Extracellular vesicles: exosomes, microvesicles, and friends. *J Cell Biol, 200*(4), 373-383.
51. Ratajczak, J., Miekus, K., Kucia, M., Zhang, J., Reca, R., Dvorak, P., & Ratajczak, M. Z. (2006). Embryonic stem cell-derived microvesicles reprogram hematopoietic progenitors: evidence for horizontal transfer of mRNA and protein delivery. *Leukemia, 20*(5), 847-856.
52. Schepers, K., Pietras, E. M., Reynaud, D., Flach, J., Binnewies, M., Garg, T., Wagers, A. J., Hsiao, E. C., Passegué, E. (2013). Myeloproliferative neoplasia remodels the endosteal bone marrow niche into a self-reinforcing leukemic niche. *Cell Stem Cell, 13*(3), 285-299.
53. Simpson, R. J., Lim, J. W., Moritz, R. L., & Mathivanan, S. (2009). Exosomes: proteomic insights and diagnostic potential. *Expert Rev Proteomics, 6*(3), 267-283.

54. Skog, J., Würdinger, T., van Rijn, S., Meijer, D. H., Gainche, L., Sena-Esteves, M., Curry Jr., W. T., Carter, B. S., Krichevsky, A. M., Breakefield, X. O. (2008). Glioblastoma microvesicles transport RNA and proteins that promote tumour growth and provide diagnostic biomarkers. *Nat Cell Biol, 10*(12), 1470-1476.
55. Svennerholm, K., Rodsand, P., Hellman, U., Waldenström, A., Lundholm, M., Ahrén, D., Biber, B., Ronquist, G., Haney, M. (2016). DNA Content in Extracellular Vesicles Isolated from Porcine Coronary Venous Blood Directly after Myocardial Ischemic Preconditioning. *PLoS One, 11*(7), e0159105.
56. Szczepanski, M. J., Szajnik, M., Welsh, A., Whiteside, T. L., & Boyiadzis, M. (2011). Blast-derived microvesicles in sera from patients with acute myeloid leukemia suppress natural killer cell function via membrane-associated transforming growth factor-beta1. *Haematologica, 96*(9), 1302-1309.
57. Taskesen, E., Bullinger, L., Corbacioglu, A., Sanders, M. A., Erpelinck, C. A., Wouters, B. J., van der Poel-van de Luytgaarde, S. C., Damm, F., Krauter, J., Ganser, A., Schlenk, R. F., Löwenberg, B., Delwel, R., Döhner, K. (2011). Prognostic impact, concurrent genetic mutations, and gene expression features of AML with CEBPA mutations in a cohort of 1182 cytogenetically normal AML patients: further evidence for CEBPA double mutant AML as a distinctive disease entity. *Blood, 117*(8), 2469-2475.
58. Thakur, B. K., Zhang, H., Becker, A., Matei, I., Huang, Y., Costa-Silva, B., Zheng, Y., Hoshino, A., Brazier, H., Xiang, J., Williams, C., Rodriguez-Barrueco, R., Silva, J. M., Zhang, W., Hearn, S., Elemento, O., Paknejad, N., Manova-Todorova, K., Welte, K., Bromberg, J., Lyden, D. (2014). Double-stranded DNA in exosomes: a novel biomarker in cancer detection. *Cell Res, 24*(6), 766-769.
59. Tkach, M., Kowal, J., & Théry, C. (2018). Why the need and how to approach the functional diversity of extracellular vesicles. *Philos Trans R Soc Lond B Biol Sci, 373*(1737).
60. Vaidya, M., Bacchus, M., & Sugaya, K. (2018). Differential sequences of exosomal NANOG DNA as a potential diagnostic cancer marker. *PLoS One, 13*(5), e0197782.
61. Valadi, H., Ekström, K., Bossios, A., Sjöstrand, M., Lee, J. J., & Lötvall, J. O. (2007). Exosome-mediated transfer of mRNAs and microRNAs is a novel mechanism of genetic exchange between cells. *Nat Cell Biol, 9*(6), 654-659.
62. Voso, M. T., Ottone, T., Lavorgna, S., Venditti, A., Maurillo, L., Lo-Coco, F., & Buccisano, F. (2019). MRD in AML: The Role of New Techniques. *Front Oncol, 9*, 655.
63. Wang, L., Li, Y., Guan, X., Zhao, J., Shen, L., & Liu, J. (2018). Exosomal double-stranded DNA as a biomarker for the diagnosis and preoperative assessment of p
64. Whiteside, T. L. (2016). Tumor-Derived Exosomes and Their Role in Cancer Progression. *Adv Clin Chem, 74*, 103-141.
65. Yáñez-Mó, M., Siljander, P. R., Andreu, Z., Zavec, A. B., Borràs, F. E., Buzas, E. I., Casal, E., Cappello, F., Carvalho, J., Colás, E., Cordeiro-da Silva, A., Fais, S., Falcon-Perez, J. M., Ghobrial, I. M., Giebel, B., Gimona, M., Graner, M., Gursel, I., Gursel, M., Heegaard, N. H. H., Hendrix, A., Kierulf, P., Kokubun, K., Kosanovic, M., Kralj-Iglic, V., Krämer-Albers, E.-M., Laitinen, S., Lässer, C., Lener, T., Ligeti, E., Linē, A., Lipps, G., Llorente, A., Lötvall, J., Manček-Keber, M., Marcilla, A., Mittelbrunn, M., Nazanrenko, I., Nolte-'t Hoen, E. N. M., Nyman, T. A., O'Driscoll, L., Oliveira, C., Pállinger, É., Del Portillo, H. A.,

Reventós, J., Rigau, M., Rohde, E., Sammar, M., Sánchez-Madrid, F., Santarém, N., Schallmoser, K., Stampe Ostenfeld, M., Stoorvogel, W., Stukelj, R., Van der Grein, S. G., Vasconcelos, M. H., Wauben, M. H. M., De Wever, O. (2015). Biological properties of extracellular vesicles and their physiological functions. *J Extracell Vesicles, 4*, 27066.

66. Yang, S., Che, S. P., Kurywchak, P., Tavormina, J. L., Gansmo, L. B., Correa de Sampaio, P., Tachezy, M., Bockhorn, M., Gebauer, F., Haltom, A. R., Melo, S. A., LeBleu, V. S., Kalluri, R. (2017). Detection of mutant KRAS and TP53 DNA in circulating exosomes from healthy individuals and patients with pancreatic cancer. *Cancer Biol Ther, 18*(3), 158-165.

7. Abkürzungen

Abkürzung	Bedeutung
AML	Akute myeloische Leukämie
AML-BFM	Akute myeloische Leukämie- Berlin-Frankfurt-Münster
APL	Akute Promyelozytenleukämie
BCA	Bicinchoninsäure-Assay
Bzw.	beziehungsweise
Ca.	circa
DNA	Desoxyribonukleinsäure
dsDNA	Doppelstrang-DNA
EV	Extrazelluläre Vesikel
EV-DNA	DNA aus extrazellulären Vesikeln
EV-RNA	RNA aus extrazellulären Vesikeln
FAB	French-American-British
FACS	Flourescence activated cell sorting
FLT3	Fms-like Tyrosin Kinase 3
gDNA	Genomische DNA
ITD	Internale Tadem-Duplikation
KM	Knochenmark
MRD	minimale Resterkrankung
mRNA	Messenger RNA
miRNA	MikroRNA
MV 4-11	Zelllinie von biphenotypischer B myelomonozytischer Leukämie
NGS	next generation sequencing
nm	Nanometer
NPM1	nucleophosmin 1
NTA	Nano Partikel Tracking Analyse
OCI-AML3	Zelllinie einer akuten myeloischen Leukämie
PCR	Polymerase Kettenreaktion
RNA	Ribonukleinsäure
TKD	Thyrosinkinase-Domäne

ZNS	Zentrales Nervensystem
µl	Mikroliter

8. Liste der Abbildungen

Abbildung 1 - Definitionen von prognostischen Gruppen aufgrund ihrer Genetik……..7

Abbildung 2 - Verteilung der verschiedenen Typ-I und Typ-II Aberrationen in der pädiatrischen AML……...9

Abbildung 3 - Biogenese von extrazellulären Vesikeln…….11

9. Danksagung

Ich bin zahlreichen Menschen ausgesprochen dankbar für all die Unterstützung, ohne die ich diese Arbeit nicht hätte, zustande bringen können.

Zuerst möchte ich meinem Doktorvater, Herrn Prof. Dr. med Dirk Reinhardt, für die Überlassung des Projekts und für die danach erfolgte Unterstützung, die Ratschläge sowie die Motivation danken.

Zudem gilt auch meinem Betreuer Prof. Dr. rer. nat. Basant Thakur großer Dank. Durch ihn bekam ich einen Einblick in die medizinische Forschung und die Chance einen Teil zu dieser beitragen zu können. Ich habe unglaublich viel von ihm gelernt und konnte stets auf seine Unterstützung zählen.

Dies gilt ebenfalls für all die Mitglieder unserer Forschungsgruppe Fr. Dr. rer. nat. Evangelia Kontopoulou, Fr. Dr. rer. nat. Katarina Reinhardt, Fr. Dr. rer. nat. Sarah Strachan, sowie Fr. Maren Soldierer, speziell für die PhD-Studenten, die mir in zahlreichen Momenten mit Rat und Tat zur Seite standen.

Mithilfe der finanziellen Unterstützung der *Jose Carreras Leukämie Stiftung* war es mir möglich, mich gänzlich dem Forschungsprojekt widmen zu können, wofür ich sehr dankbar bin.

Zum Schluss möchte in meiner Familie und meiner Partnerin danken. Für all den Glauben in meine Fähigkeiten, all das Verständnis, die Ruhe und die mentale Unterstützung, auch in schwierigen Momenten.

10. Lebenslauf

Der Lebenslauf ist in der Online-Version aus Gründen des Datenschutzes nicht enthalten.